



Norwegian University of  
Science and Technology

# Increasing power output from Francis turbines

Effektøkning i vannkraftverk med Francis turbiner

**Bente Taraldsten Brunes**

Master of Science in Product Design and Manufacturing

Submission date: December 2009

Supervisor: Torbjørn Kristian Nielsen, EPT

Norwegian University of Science and Technology  
Department of Energy and Process Engineering



# Problem Description

The main objective is to investigate potential increase in power output from the existing turbines at Ruacana Hydropower station. This is restricted by only consider a runner replacement. The technical aspect of a rehabilitation project is investigated.

Preliminary study of achievements in refurbishment projects and distribution of turbine types.

Analyze all hydraulic conditions. This entails surge oscillation and water hammer investigations for both the existing hydraulic conditions and with the aim of increasing volume flow. In addition to a review of the state of the waterway.

Use traditional turbine theory to investigate potential increase in power output.

Assignment given: 28. September 2009

Supervisor: Torbjørn Kristian Nielsen, EPT





## MASTER THESIS

for

Bente Taraldsten Brunes  
Fall 2009

### **Increasing power output from Francis turbines**

*Effektøkning i vannkraftverk med Francis turbiner*

#### **Background**

The design of turbines has undergone an evolution over the last 20 years. This has resulted in a tangible improvement potential with regard to both efficiency and turbine output.

#### **Objective**

Investigate the possibility of increasing the power output in existing hydropower plants with a focus on intermediate pressure Francis turbines.

#### **Sub objectives**

1. As a frame to a study, a mapping shall be performed on a world basis, concerning distribution of turbine type and head range for medium to large units (In a range from 50 MW). In parallel, the possibility of increasing power will be compared for different turbine types, also taking into account the head range. This may be done based on a number of representative recent upgraded hydropower plants. (This is meant as an introduction, not more than 10% of total time).
2. Use Ruacana Hydropower Station as a base to determine possible increase in output in a typical medium head Francis installation. Rucana Hydropower Plant is situated in Namibia and owned by Namibia Power Corporation Ltd. The current plant consists of 3 Francis turbines with a power output of 82.8 MW. Work has started on the installation of a fourth unit. The power situation in Namibia makes it attractive to increase the output of existing units in a next stage.
  - Analyze all hydraulic conditions for existing turbines based on available data.
  - Compare data to similar installations and also to the fourth unit being installed.
  - Based on traditional turbine theory, perform an analysis of existing conditions and of possibilities of increasing power output.
  - As far as practically possible, perform an analysis starting from a typical traditional Francis geometry, investigating possible increase in output/improvement of cavitation characteristics with a modified design. Keeping the geometry for guide vanes, stay ring/spiral and draft tube.

Senest 14 dager etter utlevering av oppgaven skal kandidaten levere/sende instituttet en detaljert fremdrift- og evt. forsøksplan for oppgaven til evaluering og evt. diskusjon med faglig ansvarlig/ veiledere. Detaljer ved evt. utførelse av dataprogrammer skal avtales nærmere i samråd med faglig ansvarlig.

Besvarelsen redigeres mest mulig som en forskningsrapport med et sammendrag både på norsk og engelsk, konklusjon, litteraturliste, innholdsfortegnelse etc. Ved utarbeidelsen av teksten skal kandidaten legge vekt på å gjøre teksten oversiktlig og velskrevet. Med henblikk på lesning av besvarelsen er det viktig at de nødvendige henvisninger for korresponderende steder i tekst, tabeller og figurer anføres på begge steder. Ved bedømmelsen legges det stor vekt på at resultatene er grundig bearbeidet, at de oppstilles tabellarisk og/eller grafisk på en oversiktlig måte, og at de er diskutert utførlig.

Alle benyttede kilder, også muntlige opplysninger, skal oppgis på fullstendig måte. (For tidsskrifter og bøker oppgis forfatter, tittel, årgang, sidetall og evt. figurnummer.)

Det forutsettes at kandidaten tar initiativ til og holder nødvendig kontakt med faglærer og veileder(e). Kandidaten skal rette seg etter de reglementer og retningslinjer som gjelder ved alle fagmiljøer som kandidaten har kontakt med gjennom sin utførelse av oppgaven, samt etter eventuelle pålegg fra Institutt for energi- og prosesssteknikk.

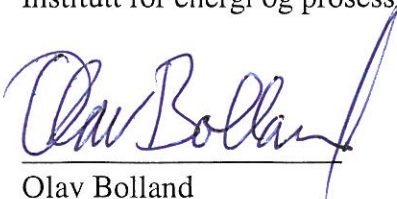
I henhold til "Utfyllende regler til studieforskriften for teknologistudiet/sivilingeniørstudiet" ved NTNU § 20, forbeholder instituttet seg retten til å benytte alle resultater i undervisnings- og forskningsformål, samt til publikasjoner.

Ett -1 komplett eksemplar av originalbesvarelsen av oppgaven skal innleveres til samme adressat som den ble utlevert fra. (Det skal medfølge et konsentrert sammendrag på maks. en maskinskrevet side med dobbel linjeavstand med forfatternavn og oppgavetittel for evt. referering i tidsskrifter).

Til Instituttet innleveres to - 2 komplette, kopier av besvarelsen. Ytterligere kopier til evt. medveiledere/oppgavegivere skal avtales med, og evt. leveres direkte til, de respektive.

Til instituttet innleveres også en komplett kopi (inkl. konsentrerte sammendrag) på CD-ROM i Word-format eller tilsvarende.

Institutt for energi og prosesssteknikk, 25. august 2009



Olav Bolland  
Instituttleder



Torbjørn K. Nielsen  
Faglærer/veileder

Medveiledere: Olof Skuncke, Multiconsult

---

# Preface

---

The presented work has been completed on the behalf of NamPower and Multiconsult. In collaboration with the Department of Energy and Process Engineering at the Norwegian University of Science and Technology (NTNU) fall 2009. The objective has been to investigate the possibility of increasing power output of an existing turbine structure by only consider runner replacement. Ruacana Hydro Power Plant in Namibia has been used as a basis for the study.

I would like to especially thank NamPower for an educational trip to Namibia in order to survey the plant and gain vital information. In addition would I like to thank Multiconsult their support. My supervisor Professor Torbjørn Kristian Nielsen have also contributed to the final results with his guidance. At last but not least, I would like to thank all the students at the Hydro Power Laboratory for their contribute to an amazing work environment.

Bente Taraldsten Brunen  
Norway, Trondheim, December 21, 2009





---

# Abstract

---

The main objective in this thesis was to investigate a potential increase of power output from the existing turbines at Ruacana Hydropower Station. This was restricted to only consider a runner replacement, and only technical aspects of a rehabilitation project has been evaluated. This involved an investigation of hydraulic conditions, limited to surge oscillation and water hammer calculations. The results was thereafter used in a calculation model to estimate potential increase in power output. Vital information about the plant and the condition of the waterway was obtained from a study trip to Ruacana.

An increase in power output in a turbine can be obtained by increasing the volume flow and/or efficiency. The first criteria can be achieved through expanding the outlet diameter of the runner, and/or altering the flow angles. Therefore has the hydraulic conditions also been analysed with the aim of increasing volume flow. It was found that it can be increased to a maximum nominal volume flow of one unit to  $85\text{m}^3/\text{s}$ . It was limited by the maximum upsurge in the Surge Headbay with the intake level at highest flood level. The restrictions are altered for the minimum water levels in the intake and maximum levels in the tailrace when operating 1 to 4 units. The advances in Francis runner design over the last decades makes an increase in efficiency feasible.

Finally a calculation method for estimating a potential increase in power output was developed. This was based on traditional turbine theory, and the aim was to find the maximum increase starting from the existing degree of submergence. In addition were the results compared to values obtained from a calculation method developed by Sintef [21].

From a preliminary study of achievements in refurbishment projects was it found that on average has an increase of 18% been obtained. The method developed in this thesis concluded that an increase of 10 – 14% in nominal power output is possible. Assuming a turbine efficiency of 0.93 and only replacing the runner. Sintef's method estimated a maximum value of 15% for the same conditions. It is also found that the outlet diameter at Ruacana can be increased by 60 mm. The additional increase in power output is only estimated to be 1% from the method developed in this thesis. The Sintef method estimates additional 3 % increase for the same scenario.



---

# Sammendrag

---

Hovedmålet med denne masteroppgaven var å undersøke muligheten for å øke effektuttak fra turbinene ved Ruacana kraftstasjon. Dette ble begrenset av kun å vurdere bytte av løpehjul. Kun tekniske vurderinger har blitt gjort, og disse bestod av å undersøke svingninger og trykkstøt. Informasjon fra dette ble videre brukt i en beregningsmodell for å estimere mulig økning i effektuttak. Denne ble basert på tradisjonell turbinteori og tok utgangspunkt i dykkingen av turbinene på Ruacana. Dette har også blitt beregnet ved bruk av en liknende metode utviklet av Sintef [21]. Verdifull informasjon om kraftverket og tilstanden til vannveien ble samlet inn under en studietur til Ruacana.

En økning av effektuttaket i en turbin kan gjøres ved å øke volumstrømmen og/eller virkningsgraden. Den første muligheten kan gjennomføres ved å utvide utløpsdiameteren på løpehjulet og/eller ved å forandre strømningsvinklene. Utviklingen av nye design metoder for Francis løpehjul de senere årene har ført til en økning i virkningsgraden.

Formålet med dette har vært å stadfeste hvor mye volumstrømmen i vannveien kunne økes uten at det går utover sikkerheten i kraftverket. Undersøkelsene viste at den nominelle volumstrømmen per turbin kan økes til  $85 \text{ m}^3/\text{s}$ . Dette ble begrenset av det største oppsvinget i svingesjakten oppstrøms med høyest vannstand i inntaket. Lavest regulert vannstand i inntaket begrenser hvor mange turbiner som kan kjøre, og når volumstrømmen økes må denne økes. Dette gjelder også for den høyeste vannstanden i utfallet og de maksimale grensene må senkes.

Resultatet av forstudien av rehabiliteringsprosjekter viste at oppnådd økning i effektuttak var på 18%. Metoden som ble utviklet i oppgaven konkluderer med at en økning i nominelt effektuttak for en turbin mellom på 10 til 14% er sannsynlig. Dette forutsetter at virkningsgraden til turbinen er 0.93 og løpehjulet byttes ut til en med høyere slukeevne. Den maksimale økningen gitt av beregningen til Sintef ble 15% med de samme betingelsene. I tegningene av turbinene ble det funnet at utløpsdiameteren kan økes med 60 mm. Et tilleggs uttak beregnet av metoden utviklet her ble kun 1%. Sintef sin metode estimerte en ekstra økning på 2%.



---

# Contents

---

<b>Preface</b>	<b>i</b>
<b>Abstract</b>	<b>iii</b>
<b>Sammendrag</b>	<b>v</b>
<b>Contents</b>	<b>vii</b>
<b>List of Figures</b>	<b>xi</b>
<b>List of Tables</b>	<b>xiii</b>
<b>Nomenclature</b>	<b>xv</b>
<b>1 Introduction</b>	<b>1</b>
<b>2 Theory</b>	<b>3</b>
2.1 System Dynamics . . . . .	3
2.1.1 Water hammer . . . . .	4
2.1.2 Surge Oscillation in Surge Tanks . . . . .	6
2.2 The Francis Turbine . . . . .	7
2.2.1 Submergence . . . . .	8
2.2.2 Calculation of NPSH . . . . .	8
2.2.3 Classic design of a Francis Runner . . . . .	9
<b>3 Preliminary Studies</b>	<b>11</b>
3.1 Refurbishment of Existing HPP . . . . .	11
3.1.1 Distribution of turbines in the world . . . . .	12
3.1.2 Achievements . . . . .	12
3.1.3 Sintef report: Potential increase of power output . . . . .	13
3.2 Runner Design . . . . .	14
<b>4 Review of Hydraulic Conditions</b>	<b>17</b>
4.1 Components upstream turbine . . . . .	18
4.2 Turbine Units 1-3 . . . . .	20
4.2.1 Other evaluated factors . . . . .	22
4.3 Components downstream turbine . . . . .	23

<b>5</b>	<b>Calculation Methods</b>	<b>25</b>
5.1	General assumptions . . . . .	25
5.2	Pressure calculation model . . . . .	25
5.2.1	Numerical equations water hammer . . . . .	25
5.2.2	Boundary conditions . . . . .	27
5.2.3	Calculation procedure . . . . .	27
5.2.4	Verification of Water hammer Model . . . . .	27
5.3	Surge Oscillation model . . . . .	28
5.3.1	System of equations: Surge Oscillation . . . . .	29
5.3.2	Worst case scenarios . . . . .	30
5.3.3	Verification of Surge Oscillation Model . . . . .	30
5.4	Increase power output . . . . .	30
<b>6</b>	<b>Results</b>	<b>33</b>
6.1	Analysis: Existing Hydraulic Conditions . . . . .	33
6.1.1	Oscillation in Surge Headbay . . . . .	33
6.1.2	Oscillation in Surge Chamber . . . . .	34
6.1.3	Pressure in front of turbine . . . . .	34
6.2	Analysis: Increasing Volume Flow . . . . .	35
6.2.1	Oscillation in Surge Headbay . . . . .	35
6.2.2	Oscillation in Surge Chamber . . . . .	36
6.2.3	Pressure in front of turbine . . . . .	36
6.3	Analysis: Increasing Power Output . . . . .	38
<b>7</b>	<b>Discussion</b>	<b>41</b>
7.1	Hydraulic considerations . . . . .	41
7.2	Power output . . . . .	42
<b>8</b>	<b>Conclusion</b>	<b>43</b>
<b>9</b>	<b>Further Work</b>	<b>45</b>
	<b>Bibliography</b>	<b>47</b>
	<b>Appendices</b>	
<b>A</b>	<b>Ruacana Hydro Power Plant</b>	<b>I</b>
A.1	History . . . . .	II
<b>B</b>	<b>Matlab Programs</b>	<b>III</b>
B.1	Water hammer Program . . . . .	III
B.2	Surge Oscillation Program . . . . .	VI
B.3	Reduction in head program . . . . .	IX
<b>C</b>	<b>Supplement Results</b>	<b>XI</b>
C.1	Verification of Simulation Models . . . . .	XI
C.2	Supplement existing hydraulic conditions . . . . .	XI
C.2.1	Surge oscillation in Surge Headbay . . . . .	XI
C.2.2	Surge Chamber Results . . . . .	XIII
C.3	Analysis: Increasing Volume Flow extention . . . . .	XV







---

# List of Figures

---

2.1	Pressure at valve with instantaneous closing time for ideal conditions . . . . .	5
2.2	x-t diagram for solving single-pipe problems [29] . . . . .	6
2.3	Components of a Francis Turbine . . . . .	8
2.4	Severe cavitation erosion on a runner . . . . .	8
2.5	Velocity diagram [7] . . . . .	10
2.6	Main dimension of a Francis Runner, axial view . . . . .	10
3.1	Turbine distribution larger than 50 MW across the world . . .	12
3.2	Visual comparison of runners at Kiambere [23] . . . . .	15
4.1	Layout of Ruacana . . . . .	17
4.2	Surge Headbay base area (not to scale) . . . . .	19
4.3	Surge Headbay walls (not to scale) . . . . .	19
4.4	Cavitation on the hub . . . . .	21
4.5	Cavitation on the trailing edge and the outer ring . . . . .	21
4.6	Cavitation on the trailing edge near the hub . . . . .	21
4.7	Exiting turbines runner blades [2] . . . . .	22
4.8	Surge Chamber dimensions [2] . . . . .	24
5.1	Illustration of waterway for water hammer calculations . . . .	26
5.2	Verification Water Hammer program . . . . .	28
5.3	Illustration of waterway used in surge oscillation calculations	28
5.4	Verification Surge Headbay load rejection . . . . .	31
5.5	Verification Surge Chamber load rejection . . . . .	31
6.1	Pressure in front of turbine, $Z_{max} = 909.3$ masl and $Q_{unit} = 71\text{m}^3/\text{s}$ . . . . .	34
6.2	Surge oscillation SH, $H_0 = 904.5$ masl $Q_{n,station} = 340\text{m}^3/\text{s}$ .	35
6.3	Surge oscillation in SC, $H_0 = 897.8$ masl and $Q_{n,station} = 340\text{m}^3/\text{s}$ . . . . .	36
6.4	Surge oscillation in SC, $Q_{n,station} = 340\text{m}^3/\text{s}$ , $H_u = 767.6$ masl . . . . .	37
6.5	Pressure in front of turbine, $Z_{max} = 909.7$ masl $Q_{unit} = 85\text{m}^3/\text{s}$	37
6.6	Percentile increase in power output as a function of volume flow and reduction in net head. For 1 turbine when 4 are in operation. . . . .	39

A.1 Ruacana Falls . . . . .	I
C.1 Verification Surge Headbay reload . . . . .	XI
C.2 Verification Surge Chamber reload . . . . .	XII
C.3 Surge oscillation at highest flood level 4 units . . . . .	XII
C.4 Surge oscillation SH, $H_0 = 895.2$ masl and $Q_{unit} = 71\text{m}^3/\text{s}$ . . . . .	XIII
C.5 Surge oscillation in SH, $H_0 = 896.4$ masl and $Q = 142\text{m}^3/\text{s}$ . . . . .	XIII
C.6 Surge Oscillation in SH, $H_0 = 897$ masl and $Q = 213\text{m}^3/\text{s}$ . . . . .	XIV
C.7 Surge oscillation in SH, $H_0 = 897.4$ masl and $Q = 284\text{m}^3/\text{s}$ . . . . .	XIV
C.8 Surge oscillation in SC, $H_u = 768$ and $Q = 284\text{m}^3/\text{s}$ . . . . .	XV
C.9 Surge oscillation in SC, $H_u = 768.3$ masl and $Q = 213\text{m}^3/\text{s}$ . . . . .	XV
C.10 Surge oscillation in SC, $H_u = 768.7\text{masl}$ and $Q = 142\text{m}^3/\text{s}$ . . . . .	XVI
C.11 Surge oscillation in SC, $H_u = 769.2\text{masl}$ and $Q = 71\text{m}^3/\text{s}$ . . . . .	XVI
C.12 Surge oscillation in SH, $H_0 = 897.5$ masl and $Q = 255\text{m}^3/\text{s}$ . . . . .	XVI
C.13 Surge oscillation in SH, $H_0 = 897$ masl $Q = 142\text{m}^3/\text{s}$ . . . . .	XVII
C.14 Surge oscillation in SH, $H_0 = 906$ masl $Q = 71\text{m}^3/\text{s}$ . . . . .	XVII
C.15 Surge oscillation in SC $H_u = 767.9$ masl and $Q = 255\text{m}^3/\text{s}$ . . . . .	XVIII
C.16 Surge oscillation in SC $H_u = 768.2$ masl and $Q = 170\text{m}^3/\text{s}$ . . . . .	XVIII
C.17 Surge oscillation in SC, $H_u = 769.2$ masl and $Q = 85\text{m}^3/\text{s}$ . . . . .	XIX

---

# List of Tables

---

3.1	Refurbished HPP with Francis turbines [28], [19], [31], [20], [23], [14], [8]	13
4.1	Intake water levels	18
4.2	Pressure tunnel data	18
4.3	Surge Headbay levels	18
4.4	Penstock data	20
4.5	Turbine unit data	20
4.6	Tailwater levels and volume flow	23
5.1	Verification: Ideal and actual values of water hammer	27
6.1	Results: analysis of existing conditions in Surge Headbay 4 units	33
6.2	Results: Analysis of existing conditions at MRWL levels	33
6.3	Results: Analysis of existing conditions in Surge Chamber	34
6.4	MRWL levels for increased volume flow	35
6.5	Maximum levels in tailrace with increased volume flow	36
6.6	Maximum percentile increase in nominal power output for one unit	38



---

# Nomenclature

---

<b>Symbol</b>	<b>Description</b>	<b>Unit</b>
$a$	Speed of sound/Acoustic speed	[m/s]
$a$	Submergence factor	–
$b$	Submergence factor	–
$A$	Cross-sectional area	$m^2$
$B$	Heigh of runner	[m]
$B$	Pipeline characteristic impedance	–
$c$	Head loss coefficient	–
$c_m$	Absolute meridinal velocity	[m/s]
$c_u$	Absolute tangential velocity	[m/s]
$D$	Diameter runner/pipe	[m]
$g$	Gravity constant	[m/s <sup>2</sup> ]
$H$	Head	[m]
$H$	Piezometer pressure	[mWC]
$H_0$	Water level at intake	[masl]
$H_u$	Water level tailrace	[masl]
$H_s$	Suction head	m
$h$	Hydraulic pressure	[mWC]
$h_b$	Barometric pressure	m
$h_{va}$	Vapour pressure	m
$h_f$	Total head loss in waterway	m
$K$	Bulk modulus	[kg/ms <sup>2</sup> ]
$L$	Length of pipe/ nearest free water surface	[m]
$n$	Rotational speed	[rpm]
$NPSH$	Net Positive Suction Head	m
$P$	Power ouput	[W]
$Q$	Volume flow	[m <sup>3</sup> /s]
$R$	Pipe line resistance coefficient	–
$t$	Time	[s]
$T$	Period	s
$T_R$	Reflection time	s
$T_L$	Closing time	s
$u$	Peripheral velocity	[m/s]
$v$	Velocity	[m/s]
$w$	Relative velocity	[m/s]
$z$	Elevation	$m$

### Greek Symbols

Symbol	Description	Unit
$\beta$	Outlet angle runner	[rad]
$\omega$	Angular velocity	[rad/s]
$\Omega$	Speed number	–
$\eta$	Efficiency	–
$\rho$	Density of water	[kg/m <sup>3</sup> ]
$\lambda$	Friction factor	

### Subscripts and Superscripts

Symbol	Description
*	BEP J <sub>eg</sub> n
1	Inlet of runner/Conduit 1
2	Outlet of runner/Conduit 2
3	Conduit 3
A	Preceding value, previous time step
B	Succeeding value, previous time step
e	Net head
min	maximum downsurge
max	maximum upsurge
m	Meridian
n	Nominal values
new	New volume flow/head
P	Current time step
station	Total volume flow station
unit	Volume flow of one unit

### Abbreviations

Symbol	Description	Unit
masl	Metres above sea level	
HPP	Hydro Power Plant	
SWAWEK	South West African Water and Electricity Corporation	
BEP	Best Efficiency Point	
HRWL	Highest-regulated water level	[masl]
HFL	Highest flood level	[masl]
NRWL	Normal draw-down level	[masl]
MRWL	Minimum draw-down level	[masl]
OP	Operating platform Surge Headbay	
GS	General section Surge Headbay	
SH	Surge Headbay	
SC	Surge Chamber	

# Chapter 1

---

## Introduction

---

Today the energy situation in Namibia is strained, and it is mainly due to the fact that the country is only able to produce about half of its consumption. The one hydro power plant is Ruacana which produces 97.8 % of total electric power production. The plant consists of three medium head Francis turbines which were commissioned in 1978. This plant serves as a basis for this thesis. The country is dependent on importing energy from the Southern African Power Pool (SAPP). This system mainly constitutes of large coal plants, and the accessibility to peak power is low.

The advancements in turbine technology have been remarkable over the last 20 years, especially within the design of Francis turbines field. It is proven to increase efficiency and improve cavitation behaviour. The result is a tangible improvement potential in efficiency and power output for existing turbines.

This thesis considers the technical aspects of a rehabilitation project. The main objective is to investigate the possibility of increasing the power output from the existing turbines by replacing the runners. This can be achieved either by increasing the volume flow and/or efficiency. The first criteria can be achieved through expanding the outlet diameter and/or altering the flow angles.

This thesis will approach the problem by investigating the existing hydraulic conditions for surge oscillation and water hammer. The selected method to solve the problem is to develop Matlab programs. The objective is to identify the maximum increase in volume flow that do not compromise the hydraulic design conditions in the waterway. The results are then used as restrictions in the developing of a calculation model for investigation of potential power output.





## Chapter 2

---

# Theory

---

The presented theory is selected on the basis of relevance for the study. It starts with system dynamics theory, and ends with a synopsis of the general turbine theory with an emphasis on runner design.

### 2.1 System Dynamics

The unsteady flow in pipelines is known as surge, and occurs due to the inertia of the water masses when changing the operating load. Any change in the volume flow changes the pressure in front of the turbine due to an acceleration or a deceleration of the water masses. The governing equations are described by the continuity equation (2.1) and the equation of motion (2.2) for a fluid element [37].

$$\frac{\partial H}{\partial t} + \frac{a^2}{g} \frac{\partial v}{\partial x} = 0 \quad (2.1)$$

$$g \frac{\partial H}{\partial x} + \frac{\partial v}{\partial t} + \lambda \frac{v|v|}{2D} \quad (2.2)$$

$H$  - Piezometer pressure ,  $h + z$  [mWC]

$h$  - Hydraulic pressure [mWC]

$z$  - Elevation [m]

$a$  - Speed of sound [m/s]

$v$  - Velocity [m/s]

$t$  - Time [s]

$\lambda$  - Friction factor

$g$  - Gravity constant  $m/s^2$

$D$  - Diameter of pipe [m]

In a waterway are the head losses due to friction and shear stresses between the water and the tunnel walls. When increasing the volume flow will the losses increase, and consequently reduces the available head for the turbine. It also makes it necessary to investigate if an existing power plant can handle the pressure change. This is usually done by investigation the surge oscillation and water hammer effects. These are treated separately,

because the period of water hammer effects in penstock are of much shorter period than surge tank fluctuations [37].

### 2.1.1 Water hammer

The volume flow in a pipeline can be viewed as a spring-mass system. The spring represents the elasticity or the compressibility of the water  $K$ , also called the bulk modulus. If a force is induced on the spring, it is compressed and represents the potential energy in the system. The elasticity and inertia of water are the causes of water hammer effects which is defined as the retardation pressure, and propagates from the turbine to the nearest free water surface upstream with the speed of sound  $a$ . For a very thick-walled pipe is  $a$  the acoustic speed of a small disturbance in an infinite fluid used, defined in equation (2.3) [37], and its value is approximately 1200m/s.

$$a \approx \sqrt{\frac{K}{\rho}} \quad (2.3)$$

$K$  - Bulk modulus [ $kg/ms^2$ ]  
 $\rho$  - Density of water [ $kg/m^3$ ]

A turbine is modelled as a valve, and the progress of the pressure in front can be easiest described when imagining a flow from a reservoir through a single pipe to a valve. For ideal conditions is this illustrated in figure 2.1. The stationary pressure line is given by the elevation in the reservoir at  $t = 0$ . The pressure in front of the turbine is a combination of the elevation pressure in the reservoir and the dynamic pressure of the water hammer.

At  $t = 0$  is the velocity  $v = v_0$  in the entire pipe in direction of the valve. When the valve closes the water masses are slowed down to  $v_0 = 0$ . Upstream the water is "unaware" of the change resulting in a gage pressure at the valve. When the pressure wave has reached the reservoir is the velocity of the water masses zero in the entire pipe length. The water flows into the reservoir with a velocity of  $v = -v_0$  due to the gage pressure. Until the pressure difference disappears and  $v = -v_0$  in the pipe. This is illustrated by the descending line in the figure, and results in a negative pressure at the valve. The negative pressure wave will propagate in the pipe to the reservoir, and at the time when the pressure equalized is denoted by the ascending line in the figure. Then the process starts again.

The pressure wave depends on the ratio between the length to the nearest free water surface upstream and the cross-sectional area of the pipe ( $L/A$ ) [29]. Thereby defining the period of the wave  $T$  in equation (2.4).

$$T = \frac{4L}{a} \quad (2.4)$$

$L$  - Length to the nearest free water surface [m]

The reflection time  $T_R$  in equation (2.5) is defined as the time the pressure wave uses to return to the turbine. The closing time of the turbine  $T_L$  should be slower than  $T_R$  in order to avoid the highest obtainable pressure defined by Joukowsky in equation 2.6. In worst case does the elasticity of water

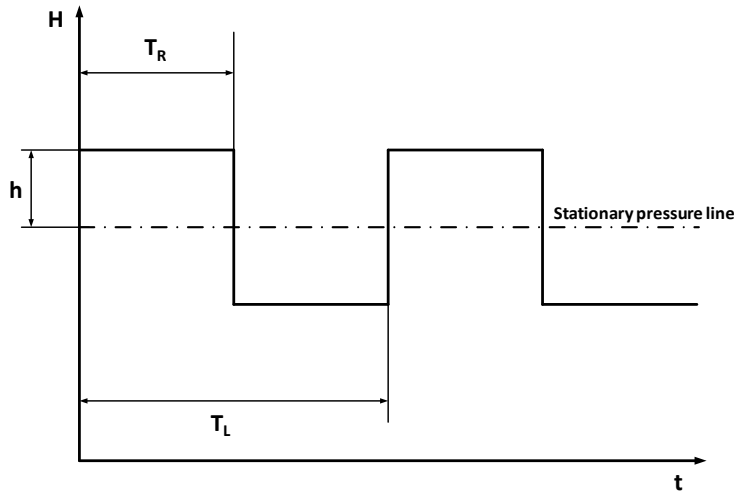


Figure 2.1: Pressure at valve with instantaneous closing time for ideal conditions

double the pressure in front of the turbine compared inelastic calculations [29].

$$T_R = \frac{2L}{a} \quad (2.5)$$

$$h = \frac{a\Delta v}{g} \quad (2.6)$$

The largest magnitude of change in volume flow per unit of time occurs during load rejection, and therefore yields the design condition in regard to the dynamic pressure [29]. It is important to solve equations (2.1) and (2.2) to find the design conditions of the pipes and valves when building a new hydro power plant. Or to check if an increased volume flow does not compromise the design in an existing plant.

### Method of Characteristics

The method of characteristics is a numerical method for solving hyperbolic differential equations in the  $xt$ -plane. It transforms the partial differential equations (PDE) (2.1) and (2.2) into ordinary differential equations (ODE) [37]. They are combined using an unknown multiplier and the result is the equations system given by (2.7) and (2.8).  $C^+$  defines the pressure wave when it propagates with the flow and  $C^-$  when the pressure wave propagates against the flow.

$$C^+ : \begin{cases} \frac{g}{a} \frac{dH}{dt} + \frac{dv}{dt} + \frac{\lambda v|v|}{2D} = 0 \\ \frac{dx}{dt} = +a \end{cases} \quad (2.7)$$

$$C^- : \begin{cases} -\frac{g}{a} \frac{dH}{dt} + \frac{dv}{dt} + \frac{\lambda v|v|}{2D} = 0 \\ \frac{dx}{dt} = -a \end{cases} \quad (2.8)$$

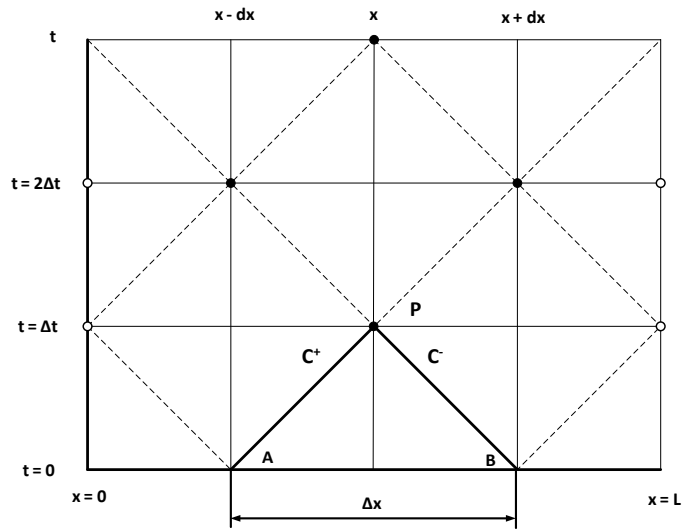


Figure 2.2: x-t diagram for solving single-pipe problems [29]

It is convenient to visualize the solution by figure 2.2 as it develops on the  $xt$  plane [37]. Where  $\frac{dx}{dt} = \pm a$  relates the change in position of a wave to the change in time by the acoustic speed  $a$ . This relationship will plot the  $+a$  straight line between A and P in which the first equation in (2.7) is valid. Between points B and P is the  $-a$  line plot and the first equation in (2.8) is valid. These lines are known as the characteristics lines.

In order to transform the equation set into finite difference equations, are equations (2.7) and (2.8) approximated by using the trapezoidal rule. The linear form of the equations are maintained, and it is a satisfactory approximation for most problems. A solution is obtained by first calculating the values for  $H$  and  $Q$  at  $t = 0$ . The calculation of the values for the next time step uses the values at the previous and so on. The resulting equation system can be found in section 5.2 along with definition of boundary conditions.

### 2.1.2 Surge Oscillation in Surge Tanks

In medium to high pressure plants it may be necessary to construct a surge chamber between the intake and the turbine. This decreases the pressure in front of the turbine, and improves the regulation of the system [29]. Due to the presence of a surge chamber the momentum of water is not destroyed quickly, but the water flows into the chamber resulting in an oscillating water level. These will eventually die out over time due to friction losses in the tunnels, losses at the inlet and in the surge chamber itself [16].

On the contrary to the water hammer the oscillation in a surge tank is slow, and the elastic effect of water has little significance. It is therefore possible to assume that water and pipes are rigid, which implies that the compressibility and thereby the speed of sound in equation (2.1) is infinite. Rearranging equation (2.10) and allowing  $a \rightarrow \infty$  in equation (2.9), the relationship in equation (2.10) is obtained.

$$\frac{\partial v}{\partial x} = -\frac{g}{a^2} \frac{\partial H}{\partial t} \quad (2.9)$$

$$\frac{\partial v}{\partial x} = 0 \quad (2.10)$$

$$g \frac{\partial H}{\partial x} - \frac{\partial v}{\partial t} + \lambda \frac{v|v|}{2D} = 0 \quad (2.11)$$

Introducing  $Q = vA$  and  $\frac{\partial H}{\partial x} = \frac{H_2 - H_1}{L}$  is the relationship (2.12) obtained:

$$\frac{L}{gA} \frac{dQ}{dt} = H_1 - H_2 - cQ|Q| \quad (2.12)$$

Where:

$$c = \lambda \frac{L}{2gA^2D} \quad (2.13)$$

Surge chambers upstream of the turbine are dimensioned in a manner to avoid both flooding for start-up load and air suction into penstock for load rejection. These should be set for worst case scenarios, i.e. when a full load rejection is followed by a full start up load at the time the shaft level is in balance with the stationary pressure line [29]. A surge chamber downstream damps strong oscillations and to prevents flooding.

## 2.2 The Francis Turbine

A Francis turbine is a radial reaction turbine and is also called a full turbine because the water completely fills the passages. The different components of the turbine are illustrated in figure 2.3.

**The spiral casing** is designed with a decreasing cross-sectional area along the circumference in order to keep the fluid velocity's magnitude constant before entering the stay vanes.

**The stay vanes/guide vanes** impart a tangential velocity onto the flow which creates an angular momentum in the water before it enters the runner. The objective is to obtain a highly uniform flow pattern with increasing rotation [7]. This is one of the main features that differentiate a Francis from other turbine types, only a part of the total specific energy at the inlet of the turbine is converted to kinetic energy before the runner is reached. The guide vanes can also be used to regulate the flow rate.

**In the runner** the energy transfer occurs due to an impulse action between the water and the blades. About 50% of the transfer is due to a pressure drop between the inlet and the outlet. The flow leaves the runner with a reduced angular momentum and a decreased pressure.

**The draft tube** connects the outlet of the runner to the tailrace. Its primary function is to reduce the velocity of the discharged water in order to minimise the loss of kinetic energy. The design of the draft tube and degree of submergence is an important design factor to avoid cavitation [7].

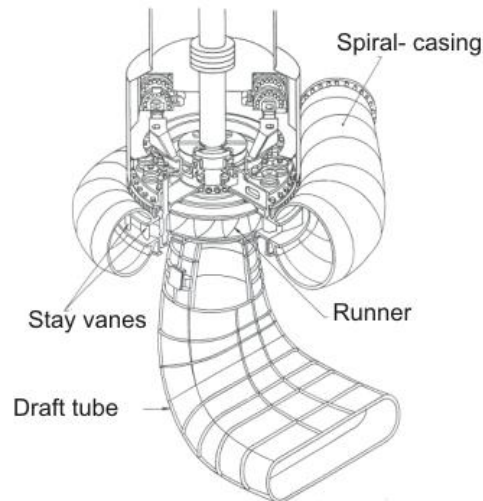


Figure 2.3: Components of a Francis Turbine

### 2.2.1 Submergence

"Cavitation form in a flowing liquid in an area where the local pressure approaches vapour pressure: entrained and dissolved gas form bubbles which grow and then collapse" [34]. This is an unstable process which gives rise to flow instability and results in noise, vibration and surface damage. The latter is also known as cavitation erosion and can sometimes alter the flow area in a runner significantly, as one can observe in picture 2.4. This usually occurs in the discharge area where the pressure is low. The commonly used method to calculate cavitation is by using the term "Net Positive Suction Head (NPSH)".



Figure 2.4: Severe cavitation erosion on a runner

### 2.2.2 Calculation of NPSH

It is normal to distinguish between  $NPSH_T$  and  $NPHS_A$  which is respectively determined by turbine characteristics in equation (2.14) and plant data

in equation (2.15) [21].

$$NPSH_T = a \frac{c_{m2}^2}{2g} + b \frac{u_2^2}{2g} \quad (2.14)$$

$a$  - Submergence coefficient

$b$  - Submergence coefficient

$c_m$  - Absolute meridional velocity at nominal load [m/s]

$u$  - Peripheral velocity [m/s]

The equation for  $NPSH_T$  yields a value for the velocity energy in the area of discharge.  $NPSH_A$  turbine is described by equation (2.15). The constants  $a$  and  $b$  are determined empirically, and depends on the speed number  $^*\Omega$  at BEP:

$$^*\Omega < 0.55 \rightarrow a = 1.12 \text{ and } b = 0.055$$

$$^*\Omega > 0.55 \rightarrow a = 1.12 \text{ and } b = 0.1^*\Omega$$

$$NPSH_A = -H_s + h_b - h_{va} \quad (2.15)$$

The suction head  $H_s$  is negative when the turbine is submerged and can be used to increase the pressure energy. The barometric pressure  $h_b = 0.13\text{m}$  at sea level decreases by  $0.12\text{m}$  for each  $100\text{m}$  above. The vapour pressure  $h_{va}$  is approximated to be  $0.3$  at  $25^\circ\text{C}$ . The criteria for avoiding cavitation is given in equation (2.16) [7].

$$NPSH_T < NPSH_A \quad (2.16)$$

### 2.2.3 Classic design of a Francis Runner

There are a number of methods to design a Francis runner. The following is a brief presentation of H. Brekke's method described in "Pumps & Turbines" [7].

The design procedure starts by determining nominal head  $H_n$  and volume flow at best efficiency point (BEP) denoted by  $^*Q$ . It is convenient to start by designing the outlet. A peripheral velocity  $u_2$  and meridian velocity  $c_{m2}$  is selected based on equation (2.14). The value of  $u_2$  lies between  $35$  and  $43$  m/s, where the highest value indicates high head. The correlation between these velocities can be seen in figure 2.5, the solid lines represent the velocity diagrams at BEP and the dotted lines represents flow past BEP. It is important to notice that the outlet angle  $\beta_2$  does not change for the different flows and the absolute tangential velocity  $^*c_{u2} = 0$  and  $\alpha_2 = 90^\circ$  at BEP. The outlet angle can therefore be determined by equation (2.17).

$$\beta_2 = \tan^{-1} \left( \frac{^*c_{m2}}{u_2} \right) \quad (2.17)$$

The outlet diameter is found from the relationship given by equation (2.18). It is then used to find the rotational speed of the runner in equation (2.19). The rotational speed must be corrected to obtain synchronous speed in order to connect the generator to the grid. Accordingly correct the outlet diameter and the other preceding values. Final step is to select a point along

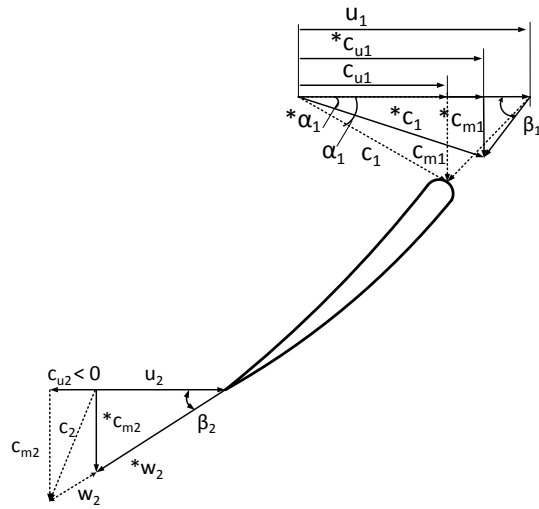


Figure 2.5: Velocity diagram [7]

the hub where the blades are finished and determine the blade angles from the assumption of perpendicular outlet.

When designing the inlet it is important to bear in mind that the inlet angle depends on the volume flow, as seen in figure 2.5. For medium and low pressure turbines is  $c_{m1}$  not constant over the inlet due to large differences between the hub and ring. Because the flow starts to curve in front of the runner.

$$*c_{m2} = \frac{4*Q}{\pi D_2^2} \quad (2.18)$$

$$u_2 = \frac{\pi D_2 n}{60} \quad (2.19)$$

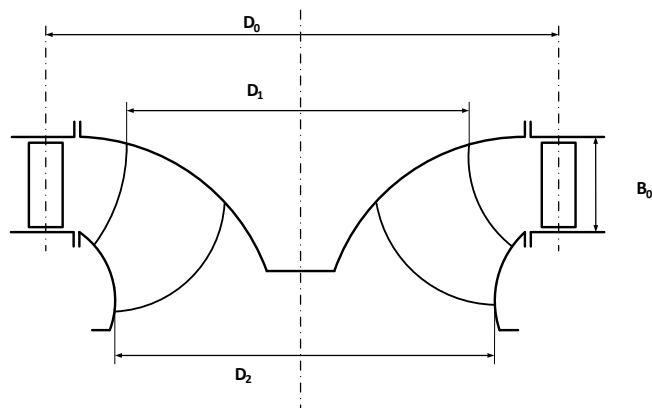


Figure 2.6: Main dimension of a Francis Runner, axial view



## Chapter 3

---

# Preliminary Studies

---

The first preliminary study focuses on motivation for refurbishment projects for hydro power plants. It also presents a percentile distribution of turbine types in the world. This is followed by achieved increase in power output and efficiency for known plants. The second study presents new advancements concerning Francis runner design.

### 3.1 Refurbishment of Existing HPP

More than 50% of old power plants has operational problems such as cavitation erosion and vibration of the structure [17]. The paramount objectives of a rehabilitation project are to maximise output, efficiency and thereby the annual energy production. An advantageous effect is reduced operating and maintenance costs, which in the end extends the plants operating life.

A rehabilitation project is often motivated by the necessity to replace key components that are at the end of their lifetime. Or a requirement to adapt the hydraulic characteristics of a turbine to new operating conditions. Nowadays this is often the case since many energy markets in the world are deregulated. The majority of plants in the western world were built before deregulation, and are now operated in order to meet the energy demands known as hydro peaking. This implies frequent operation outside the best efficiency point (BEP). This entails decreased efficiency and in some cases increased wear and tear on the plants. A side effect of the hydro peaking is that it also causes strong variations in the river flow, which in turn affects the ecological environment. This introduces the demand for regulation schemes with the smallest amount of impact on the surrounding environment. Work has started to map the effect of hydro peaking in Norway [9]. In Africa it is not an unfamiliar problem. Where the water flow varies strongly with the seasons and the demand for water for domestic and irrigation purposes is high [1].

Any rehabilitation project has to be economically justified. Not only must the cost of the project be considered, but also the cost of down time. Often does this aspect determine the rehabilitation scenario. It has been common practice to limit the rehabilitation for small to medium turbines

to only consider a replacement of the runner. Whilst for large units an optimisation of the entire hydrological profile is viable [17], [32].

#### 3.1.1 Distribution of turbines in the world

An initial survey of the distribution of turbine units rating over 50 MW across the world is presented in figure 3.1 [10] [11]. The Francis turbine has the highest percentile distribution on each continent, closely followed by the Pelton turbine. Africa has the highest number of pumped storage schemes, and to no surprise few Kaplan turbines are presented.

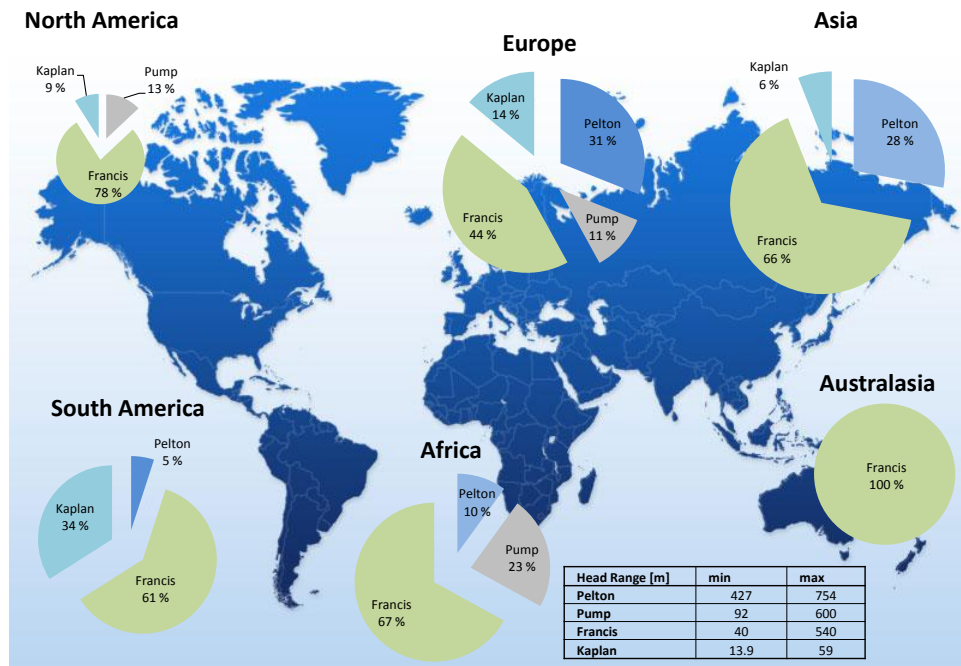


Figure 3.1: Turbine distribution larger than 50 MW across the world

#### 3.1.2 Achievements

There has been a significant increase in refurbishment projects the last decades. Some of these are finished, but only a few have published their accomplished results with adequate information.

Besides all the challenges of rehabilitation projects, does some claim that a new designed runner installed inside existing turbine structures can improve power output by 10 to 30 percentage points [33], [17], [36]. On the other hand does Andritz Hydro post a more conservative statement, the power output can be increase by 10 to 15% when modernizing and refurbishing existing turbines and generators [19].

An example of a nearly finished refurbishment project is the six Francis turbines at the Akosombo plant in Africa. In the beginning it was claimed that the following results could be achieved [19]:

- Cavitation-free performance within the full operating range
- Increase of annual energy production by 20%
- Increase of average maximum output by 18%
- Increase of peak efficiency by 5%
- Increase of full load efficiency by 5%

Unit 1 is now commissioned and field tests show that the guaranteed increase in efficiency of 5 % has been reached [14]. The refurbishment of Badu Ozzana power plant (Taloro II) in Italy is finished. The two Francis turbines built in 1960 never met their warranted performances although several modifications were performed. All main components of the turbine were replaced and site test confirmed an improvement of 4% in efficiency and nearly 15% increase in power output [19]. Statkraft has started the work of rehabilitating a large part of their hydro power plants in Norway. About 21 units have been refurbished, and on average they have achieved an increase in efficiency of 2.3% [35].

Table 3.1 presents an overview of refurbished power plants with Francis turbines. The averaged increase in power output is 18 %. Additional information about the plants can be found in Appendix D, which also includes refurbished Pelton and Kaplan turbine. Including these the total average increase in power output is 20%.

Plant	Output [MW]		
	Old	New	Increase [%]
La Villita	76	82	8
Guri II	610	715	17
Kiambere	72	84	17
Pantabangan	51.6	60.4	17
Ambuklao	25	35	40
Taloro II	13.6	15.6	15
Harsprånget	117	140	20
Kilforsen	100	120	20
Bajina Basta	95.4	108	13
Nedre Vinstra	50	65	30
Mequinenza	80.9	102	26
Såheim	54	60	11
Songa	120	136	13
<b>Average increase in power output</b>			<b>18</b>

Table 3.1: Refurbished HPP with Francis turbines [28], [19], [31], [20], [23], [14], [8]

### 3.1.3 Sintef report: Potential increase of power output

The report "Calculation of potential increase of power output in Norwegian hydro power plants" [21] presents a method in which a potential increase in

power output can be estimated. The main idea is to increase the volume flow through the runner without adding to the cavitation risk. The dimensions of the runner is increased, but limited to fit inside an existing turbine without major alterations. It is made larger by increasing the outlet diameter  $D_2$  and is limited by the cast-in diameter of the draft tube. For a Francis turbine it is not possible to increase  $D_2$  significantly without large alterations upstream the runner. This relates especially to low pressure turbines, because it affects the stay and guide vanes in addition to the draft tube. The objective is to ensure that it is only necessary to replace the lower cover and the upper part of the draft tube along with the runner.

The new  $D_2$  is either equal to the cast-in diameter or calculated using equation (3.1) by Siervo and Leva [13]. The smallest diameter is selected and the existing efficiency of the turbine in question is used. The results do not take into account a likely increase in efficiency due to a new and improved runner. The reduction in available head due to increased head losses for increased volume flow is not accounted for in the results. It is included at a later stage.

$$D_{2,new} = \left( 1.10 + \frac{(0.80 - \Omega)}{6} \right) D_2 \quad (3.1)$$

## 3.2 Runner Design

Over the last decades there has been made great headway in runner design of the Francis turbine. The new design philosophy differs from the old with an increased curvature of the blade along with a curved shape of the trailing edges [17]. The revolution within computer capacity has made it possible to go from graphically based design to a virtual method with the aid of tools such as computational fluid dynamics (CFD). This also makes it possible to numerically analyze the performance of a runner before building it. The results are proven to be in fairly good agreement with measured data [30]. The design method using CFD usually starts out with an initial guess of the runner geometry based on traditional 1D or 2D potential flow theory such as Euler. It is subsequently followed by an optimization process where the design is adjusted in order to obtain the desired characteristics [33]. The traditional theory represents the direct design method where the flow field is determined by a given blade shape. In recent years, there has been an increased interest in using an inverse design method for the initial guess. The desired characteristics of the flow field are used to determine a suitable blade geometry [4].

Another major advance is the introduction of pressure balanced blades with skewed outlets named the "X-blade". It has made it possible to stabilize dynamic behaviour and improve efficiency during off-design point [6]. X-blade has been successfully installed at Kiambere HPP in Kenya and the difference between the old and the new runner is seen in figure 3.2. The result of the project is cavitation free operation and an increase in power output of 17% [23]. Site tests are scheduled to commence spring 2010.

Runner replacements are a great hydraulic design challenge because of the geometrical constraints of the existing machines [36]. An increase in



(a) Old runner



(b) New X-blade runner

Figure 3.2: Visual comparison of runners at Kiambere [23]

power output can be obtained by increasing efficiency and/or increasing the flow rate [32], [17], [21], [19]. Improvement of cavitation behaviour can be obtained by increasing the runner outlet diameter and decrease the outlet angle. "A fully pressure balanced blade must have increased angles near the inlet in order to obtain an increased pressure towards the band" [6]. This phenomenon is easiest explained referring to equation 5.25. A large diameter reduces the blade outlet angle  $\beta_2$  which in turn reduces the required submergence. In a medium head turbine it is normal that the value of  $\beta_2$  is in the range from  $13^\circ$  to  $18^\circ$ . For the blade inlet angle  $\beta_1$  is a normal value in the range  $50^\circ$  to  $70^\circ$ . These angles have significant influence on the meridian cross section of the crown and the shroud [5].

Another geometric parameter that influences the cavitation characteristics is the blade curvature. In a successful designed runner the cavitation bubble collapses in the water downstream the blades. This is achieved by increasing the curvature of the blade letting the convex suction side have increased velocities. Especially if this is done towards the blade outlet the separation and cavitation is moved downstream [5].

The blade outlet geometry also affects the pressure oscillation in the draft tube. A skewed outlet (i.e. not radial) is proven to have a stabilizing effect. This may be due to the fact that the blade outlets are located at a smaller diameter from the crown, and a more harmonic pressure surge at part load is observed. Low pressure regions at the shroud in the inlet may be due to its curvature and can be compensated for by changing the blade lean angle [5].



## Chapter 4

---

# Review of Hydraulic Conditions

---

This review of the condition of the waterway at Ruacana is based on data submitted by NamPower, in addition to the tender documents for the construction of the new 4<sup>th</sup> Unit. A review of the available machine drawings [2] is performed in order to determine the as-built data. Information about the conditions of the waterway was also obtained through interviews with A. Espag [15] and E. Kleinhansen [24]. The components that have not experienced any particular problems are not described in detail. The general layout of Ruacana can be seen in figure 4.1, and the following presents the components of the power plant starting at the top. Background information about Ruacana can be found in appendix A.

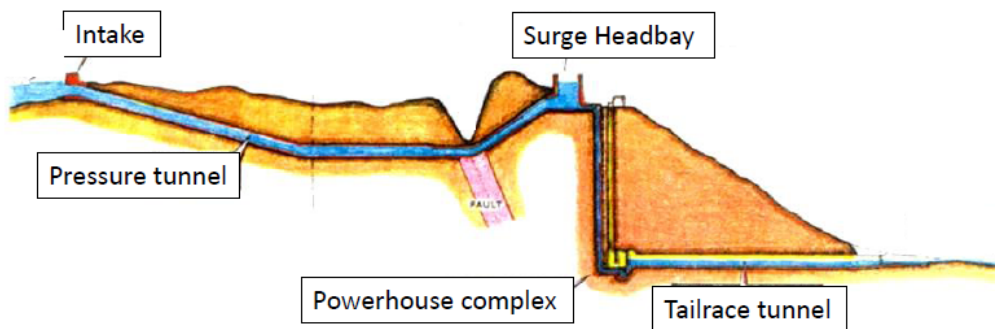


Figure 4.1: Layout of Ruacana

## 4.1 Components upstream turbine

### Diversion Weir and Pressure Tunnel

The plant is a run-of-river power plant with an intake in the shape of a diversion weir. Table 4.1 presents the headwater levels which varies strongly with the seasons and determines the regulation of the plant. At minimum draw-down level the operation of the power plant is restricted to one unit due to surge problem. The diversion weir has been drained and inspected once and no major faults were found. The water is then diverted into the pressure tunnel, which has only experienced a leakage problem due to maintenance error. Its data is presented in table 4.2.

Level, [masl]	Significance
904.5	Highest flood level
902.7	Highest regulated water level (HRWL)
901.0	Normal draw-down level (NRWL)
895.2	Minimum draw-down level (MRWL)

Table 4.1: Intake water levels

Component	Length [m]	Diameter [m]
Pipe 1	1215	8.3
Pipe 2	285	7.4
<b>Total</b>	1500	
Head loss coefficient, c	$5.2 \cdot 10^{-5}$	

Table 4.2: Pressure tunnel data

### The Surge Headbay

The dimensions of the Surge Headbay are found in drawing "No. 32 H 39e, Surge Headbay, penstock intake walls" [2]. The base area at level 882.5 masl is illustrated in figure 4.2 and the walls in figure 4.3. The walls are divided into a general section (GS) and an operating platform (OP). The OP section protrudes into the cross-sectional area up to a level of 907 masl. In the Surge Headbay have there not been found any major faults during inspections. The indicated levels in figure 4.3 are identified in table 4.3. For the air suction level a safety factor is included.

Level, [masl]	
909.7	Top level
907	Top level for Operating Platform
905	Air intake for Penstock
891.5	Calculated air suction level
882.5	Bottom level of Surge Headbay

Table 4.3: Surge Headbay levels



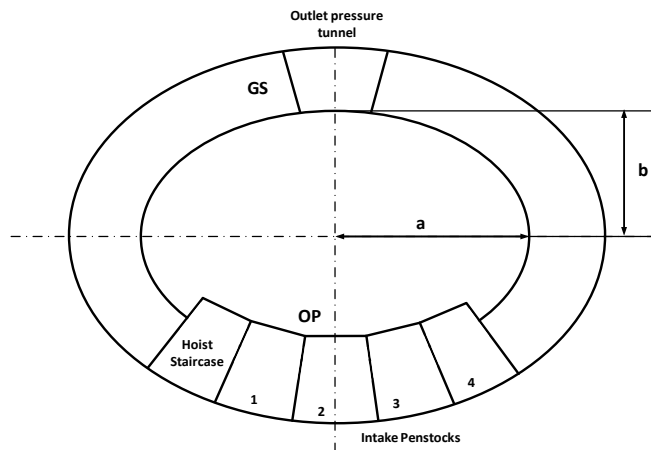


Figure 4.2: Surge Headbay base area (not to scale)

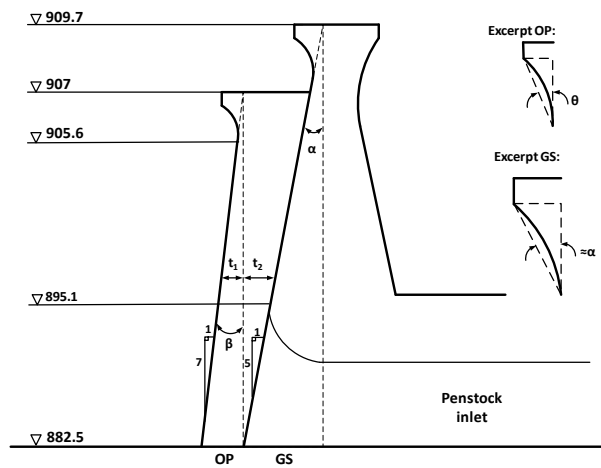


Figure 4.3: Surge Headbay walls (not to scale)

### Penstock

After the Surge Headbay the waterway divides into four penstocks that are all identical, and the data is presented in table 4.4. They are regularly inspected but no significant problem other than some paint peeling is found.

Component	Diameter	Length
Vertical:	3.6 m	120 m
Horizontal:	3.6 m	55 m
Head loss coefficient, $c$	$6.5 \cdot 10^{-4}$	

Table 4.4: Penstock data

## 4.2 Turbine Units 1-3

At the present three turbines are installed, and the process of installing the fourth unit has started. The plant was comisioned in 1978 and the existing turbine unit data are presented in table 4.5.

Manufacturer	Vöest Alpine
Number of Units	3
Nominal Output pr. turbine, $P_n$	82 MW
Nominal discharge, $Q_n$	$68 \text{ m}^3/\text{s}$
Nominal head, $H_n$	134.0 m
Rotational speed, $n$	230.8 rpm
Direction of rotation	Counter clockwise
Inlet diameter, $D_1$	3734 mm
Outlet diameter, $D_2$	2940 mm
Inlet height, $B_0$	650 mm
Number of blades, $z$	13
Internal head loss to draft tube exit, $c_t$	$0.4 \cdot 10^{-4}$

Table 4.5: Turbine unit data

### Cavitation problems

The hub experiences cavitation erosion in the area as seen in picture 4.4. It is not advantageous that it is made of cast iron. The problem has not been considered to be serious enough to repair.

The runner experiences cavitation in the discharge area along the entire trailing edge which can be observed in pictures 4.5 and 4.6. These areas are inspected and measured each year and are at the present not considered to yield any significant problems. The cavitation affects the regulation of the turbine and forced air admission in the draft tube is used in the range of 35 – 40 MW and 70 – 80 MW. The turbines are normally operated at 80 MW and can run up to 83 MW during emergencies, but then it is not possible to avoid cavitation by using forced air admission. The cause of the cavitation is not easily determined, but it is possible to rule out the  $NPSH_A$  of the system. During the construction of the power station, the "normal" high tailwater level was assessed to be 764.7 masl for a total volume flow of  $225 \text{ m}^3/\text{s}$ . This yields a submergence of  $H_s = 8.5\text{m}$ , and a total  $NPSH_A = 17.5\text{m}$  according to equation (2.15). The tailwater level varies with the volume flow and it has been deemed sufficient to subtract 15% from  $NPSH_A$  for future calculations. The nominal volume flow used in calculations today is  $284 \text{ m}^3/\text{s}$  for four units.



Figure 4.4: Cavitation on the hub

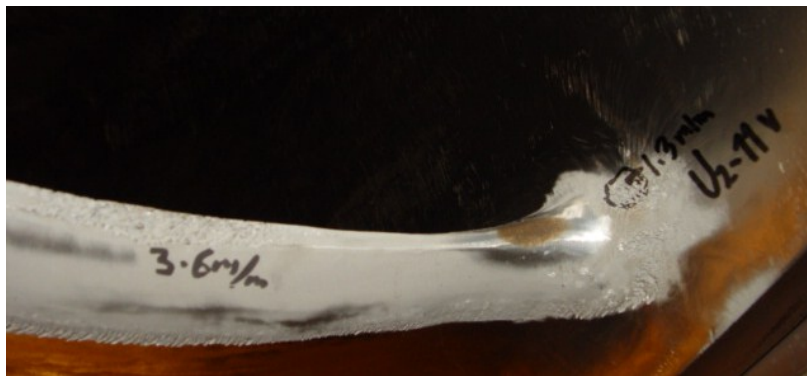


Figure 4.5: Cavitation on the trailing edge and the outer ring



Figure 4.6: Cavitation on the trailing edge near the hub

This degree of submergence should be sufficient, and therefore it is probable that the cavitation problem is due to the design of the runners. Unfortunately there does not exist sufficient information about the existing runner design in order to establish a detailed picture. The main dimensions are presented in table 4.5, and figure 4.7 presents an extract of the only available machine drawing of the runner blades "MB9-048 1109 A, Runner" [2]. From discussions with Ole Gunnar Dalhaug it has been pointed out that the pressure distribution in the inlet may cause the cavitation problem in the outlet [12]. It is therefore probable that with a new design of the runner the cavitation problems may vanish.

### 4.2.1 Other evaluated factors

A replacement of the stay ring/wicket gate is out of the question. The stay ring is quite thick, because it supports the thrust bearing. In the beginning there were many problems with the thrust bearing, and the turbine could not operate over 70 MW. It was replaced and the problems disappeared. The guide vanes and the draft tube are also regularly inspected but there have not been any notable problems. In the spiral casing the allowable pressure is 178 mWC [25]. The new unit in comparison to the existing turbines has a smaller outlet diameter and consequently a higher rotational speed. In order to be able to compare the units at Ruacana to similar installations it has been very difficult to obtain adequate information. For the turbines is  $n_{12} \approx 59$  at Ruacana. A comparison with the power plants presented in 3.1 it is found that the power plants with similar values have obtained an average increase in output of 19%.

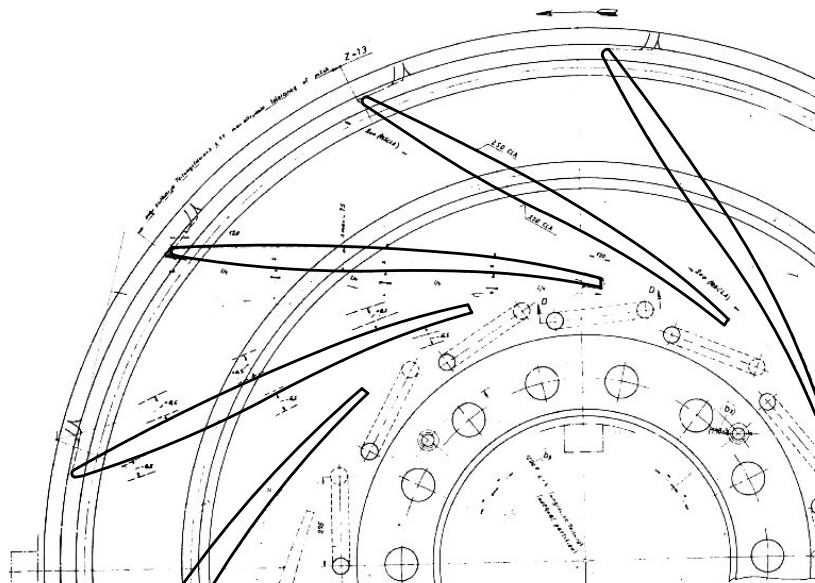


Figure 4.7: Existing turbines runner blades [2]

### 4.3 Components downstream turbine

#### Surge Chamber and Tailrace

The discharge from the four turbines are joined in the Surge Chamber, before it is lead out into the open through the tailrace. The shape and measured cross-sectional area is presented in figure 4.8, which is taken from drawing "0-42/375 rev. 5 Surge Chamber General Arrangement" [2]. The Access Gallery leads down to the main station hall, and therefore the upsurge level is of particular interest for the safety of the plant. This is denoted in the figure as "permissible flood water level" at 775 masl. During inspections neither the Surge Chamber nor the Tailrace has been subjected to any notable maintenance problems.

The tailwater level results from a combination of head loss in the tailrace tunnel and the rise in water level in the river outside the tunnel exit. The water level in the river is difficult to determine because it depends on the average flow in the river over a period of time. Table 4.6 presents the identified tailwater levels corresponding to the volume flow in the station. The last entry is fairly representative for conditions at normal high water level in the river. Drawing a straight line between the two middle measurements an incline of approximately 0.003 is obtained. This yields an acceptable relationship for the water rise in the tunnel:  $\Delta h = 0.003Q_{station}$ . The highest flood level in the tailwater is 769.2 masl.

Water level, [masl]	Volume flow, [m <sup>3</sup> /s]	
761.0	0	Measured level after stop for 12 hours
762.6	68	Measured level, one unit in operation
762.8	136	Measured level, two units in operation
764.5	225	Assessed level during construction

Table 4.6: Tailwater levels and volume flow

#### 4 Components downstream turbine

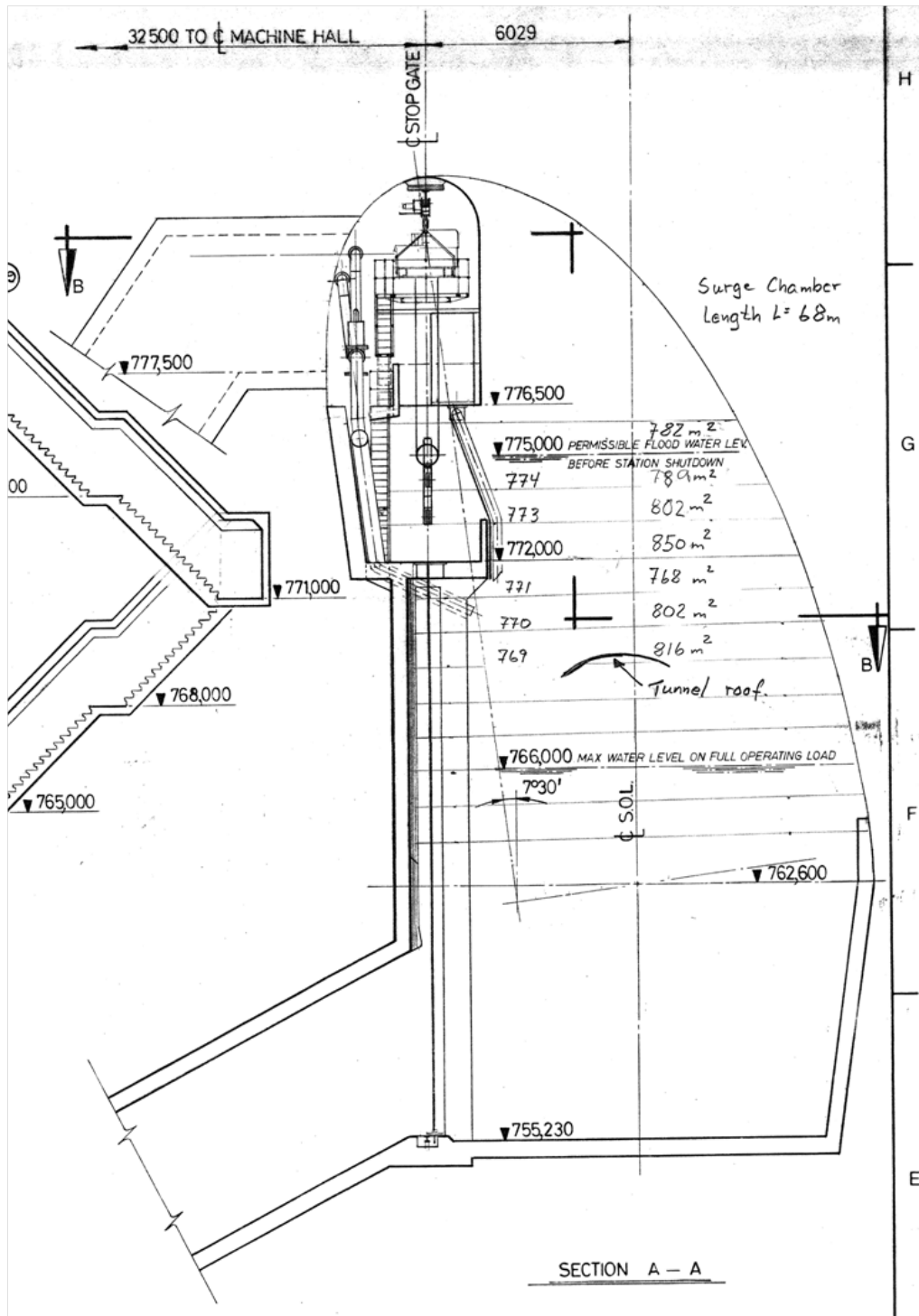


Figure 4.8: Surge Chamber dimensions [2]

## Chapter 5

---

# Calculation Methods

---

This section presents the calculation methods for water hammer and surge oscillation. Finally, a calculation model for investigating possible increase in power output is presented.

### 5.1 General assumptions

The cross-sectional area in the Surge Headbay is calculated based on figures 4.2 and 4.3. A table is generated which contains the area from the base to the top with an increment of 0.1m in the Matlab. The cross-sectional area of the Surge Chamber is found in figure 4.8. For the calculations at time  $n+1$  it is assumed sufficient to use the area corresponding to the surge level at time  $n$ .

### 5.2 Pressure calculation model

A Matlab program is developed to calculate the pressure at Ruacana, and it is presented in appendix B.1. The following presents the system of equations based on the existing conditions at Ruacana which is simplified according to figure 5.1. It is the free surface of the Surge Headbay that affects the pressure wave. It can in part be regarded as an extension of the theory presented in section 2.1.1. All of the four penstocks are identical which means that the water hammer is the same for each turbine since they are all opened and closed in the same manner [3].

#### 5.2.1 Numerical equations water hammer

The resulting numerical equation system from applying the trapezoidal rule on equations (2.7) and (2.8) is given by equations (5.1) and (5.2). Where the subscript  $P$  denotes the value at the current time step,  $A$  refers to the preceding value at  $x - dx$  and  $B$  to the succeeding value at  $x + dx$ .

$$C^+ : H_P = H_A - B(Q_P - Q_A) - RQ_P|Q_A| \quad (5.1)$$

$$C^- : H_P = H_B + B(Q_P - Q_A) + RQ_P|Q_B| \quad (5.2)$$

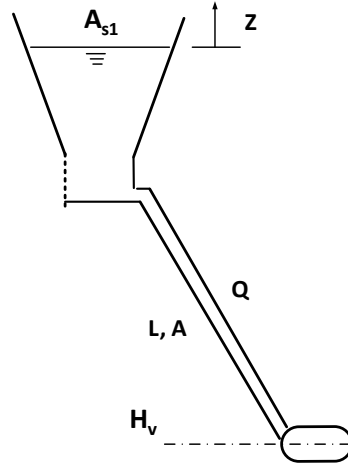


Figure 5.1: Illustration of waterway for water hammer calculations

$B$  is known as the pipeline characteristic impedance, and is given by equation (5.3).  $R$  is the pipeline resistance coefficient over the stretch  $\Delta x$  and it is here defined as in equation (5.4) due to the known head loss coefficient given in 4.

$$B = \frac{a}{gA} \quad (5.3)$$

$$R = c \quad (5.4)$$

Further discretisation of equations (5.1) and (5.2) are done by separating these into equations for  $H$  and  $Q$  in (5.5) and (5.6). A solution can be obtained for each interior point  $P$  at  $(x)$  in which the values  $C_A$ ,  $C_B$  and  $Q_R$  are known and defined by equations (5.7) – (5.9).

$$H(x, n) = \frac{1}{B} (C_A - BQ_R) + \frac{1}{B} C_B \quad (5.5)$$

$$Q(x, n) = \frac{1}{B} (H(x, n) - C_B) + Q(x + dx, n - 1) \quad (5.6)$$

$$C_A = H(x - dx, n - 1) - RQ(x - dx, n - 1) |Q(x - dx, n - 1)| \quad (5.7)$$

$$C_B = H(x + dx, n - 1) + RQ(x + dx, n - 1) |Q(x + dx, n - 1)| \quad (5.8)$$

$$Q_R = Q(x + dx, n - 1) - Q(x - dx, n - 1) \quad (5.9)$$



### 5.2.2 Boundary conditions

At  $H(x_0, n)$  the piezometer pressure is defined by the surge oscillation in the Surge Headbay as in equation (5.10). The volume flow is calculated from equation (5.6).

$$H(x_0, n) = Z(n-1) + dt \frac{Q(x-dx, n-1) - Q(x+dx, n-1)}{A_{s1}(n-1)} \quad (5.10)$$

In this system the turbine is set to behave as a valve, and the volume flow through the turbine is defined by equation (5.11). The valve elevation is used as the reference datum where the flow discharges to the atmosphere. The pressure is calculated according to equation (5.13).

$$Q(L, n) = -0.5BC_V + 0.5\sqrt{(BC_V)^2 + 4C_VC_P} \quad (5.11)$$

$$C_V = \frac{(\kappa Q_n)^2}{H_n} \quad (5.12)$$

$$H(x, n) = \left( \frac{Q(x, t)}{\kappa Q_n} \right)^2 H_n \quad (5.13)$$

### 5.2.3 Calculation procedure

The calculation procedure is [29], [37]:

1. The conduit is divided into partitions determined by the relationship  $\Delta x = a\Delta t$ . In order to obtain boundary conditions at the ends  $\frac{L}{\Delta x}$  must be a positive integer.
2. Initial values at  $t = 0$  for Q and H are calculated at each interior point and stored.
3. The equation system described in 5.2.1 and 5.2.2 is solved thereafter for time steps determined by dt.

### 5.2.4 Verification of Water hammer Model

	<b>Analytic</b>	<b>Numeric</b>	<b>Deviation</b>
$T_L$	0 s	0.0042 s	0.0042 s
$T_R$	0.34 s	0.33 s	0.1 s
p	0.6 s	0.6 s	0 s
$\Delta h$	855.9 mWC	855.8 mWC	0.1 mWC

Table 5.1: Verification: Ideal and actual values of water hammer

The water hammer program is verified by calculating the flow field without losses, and the results are shown in figure 5.2. In the figure the closing time of the valve is  $T_L = dt = 0.0042s$ , and it is shorter than the reflection time of a pressure wave  $T_R$  calculated by equation (2.5). The

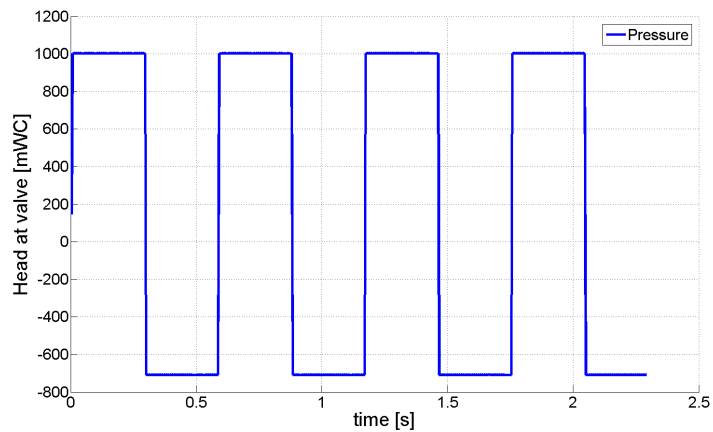


Figure 5.2: Verification Water Hammer program

pressure in the Surge Headbay is set to be constant. In table 5.1 are the ideal analytic values according to the theory in 2.1.1 presented along with the values found in the graph. This represents the numerical error in the Matlab program.

### 5.3 Surge Oscillation model

The developed Matlab program which investigates the surge oscillations levels in both surge tanks by using an Euler code is found in appendix B.2. Figure 5.3 represents the simplified waterway system at Ruacana used in the surge oscillation calculations. Here is the pressure tunnel assumed to consist of one tunnel. A weighted cross-sectional area of  $51.99 \text{ m}^2$  is used. In addition, the four penstocks are assumed to be one.

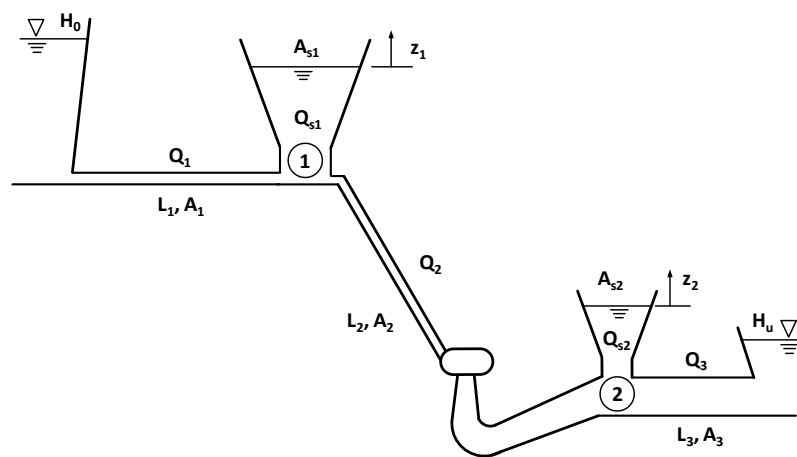


Figure 5.3: Illustration of waterway used in surge oscillation calculations

### 5.3.1 System of equations: Surge Oscillation

Equations 5.14 to 5.21 are linear partial differential equations used to solve surge oscillation in the two surge tanks illustrated in figure 5.3 [16] [29]. A solution can be obtained by using an Euler code in Matlab. As a basis for the equations is it important to note the following assumptions:

1. The elastic effect of the water is neglected because these types of oscillations are slow and therefore the change volume flow is slow.
2. The masses of the shafts are neglected. Therefore is the pressure in intersection 1 equal to the water level in surge tank 1, and the pressure in intersection 2 equal to the water level in surge tank 2.
3. Compressibility effects are not significant.

$$\frac{dQ_1}{dt} = \frac{gA_1}{L_1} (H_0 - z_1 - c_1 Q_1 |Q_1|) \quad (5.14)$$

$$\frac{dQ_2}{dt} = \frac{gA_2}{L_2} \left( z_1 - z_2 - H_n \left( \frac{Q_2}{\kappa Q_n} \right) - c_2 Q_2 |Q_2| \right) \quad (5.15)$$

$$\frac{dQ_3}{dt} = \frac{gA_3}{L_2} (z_2 - H_u - c_3 Q_3 |Q_3|) \quad (5.16)$$

Where the general equation for head loss coefficient  $c$  is given in equation (5.17)

$$c = \frac{fL}{2gA^2D} \quad (5.17)$$

For the waterway system at Ruacana are measured values used. The continuity equations (5.18) and (5.19) describe the relation between the surge shafts and tunnels. Respectively in intersections 1 and 2 in figure 5.3.

$$Q_{s1} = Q_1 - Q_2 \quad (5.18)$$

$$Q_{s2} = Q_2 - Q_3 \quad (5.19)$$

The water level in the surge tanks are given by equations (5.20) and (5.21). These equations are solved with an Euler code in Matlab, and the program is presented in appendix B.2.

$$\frac{dz_1}{dt} = \frac{1}{A_{s1}} Q_{s1} \quad (5.20)$$

$$\frac{dz_2}{dt} = \frac{1}{A_{s2}} Q_{s2} \quad (5.21)$$

### 5.3.2 Worst case scenarios

The water flow of the Kunene river is highly dependent on the season and flood conditions, and must be taken into account when determining the worst case scenarios.

The objectives of the simulations of the Surge Headbay are:

- Ensure that the water does not rise over the top of the Surge Headbay at a level of 909.7 masl.
- Avoid suction of air into the penstock. This happens if the water recedes the level of 895.1 masl .

All simulations of surge oscillation starts by rejecting from nominal volume flow  $Q_n$  down to zero. In order to find the maximum up- and downsurge is this followed by reloading of one turbine and a subsequent rejection at the worst possible time. Later this is referred to as a reload/reject sequence. For 4 units in operation at existing conditions is the nominal volume flow  $Q_n = 284\text{m}^3/\text{s}$ , and 1 unit  $Q_{n1} = 71\text{m}^3/\text{s}$ . The valve is closed using an admissions degree which is defined as  $\kappa Q_n$ . This entails that for one turbine when 4 units are in operation is the reload/reject sequence run up to 0.25, for one turbine when 3 units are in operation 0.33 and so on. The fastest operation time for reload/reject sequence of one unit is at minimum 3 minutes. The tailwater level is calculated according to  $H_u = 0.03Q_0 + 764$  masl.

The objective for the simulations of the Surge Chamber is to ensure that the water does not exceed the maximum permissible water level of 775 masl. Only the upsurge is critical to the station. Because a downsurge will only lead to a transition between submerged and free water surface conditions in the tailrace tunnel. The worst case scenario is when the level in the tailrace is at flood level of 769.2 masl. Reload/reject sequences should also be evaluated.

### 5.3.3 Verification of Surge Oscillation Model

The surge program is verified by calculating the flow field without losses and using an infinite constant cross-sectional area of 28,550 m<sup>2</sup> in the Surge Headbay and 436,880 m<sup>2</sup> in the Surge Chamber. The result for load rejection in the Surge Headbay is shown in figure 5.4 and figure 5.5. The results of reload for both chambers can be found in appendix C.1. The calculations show that the oscillation levels exceeds all limits because the system is not damped by head losses. This is also the case when looking at the curves for reload in the Surge Headbay in figure C.1 and in the Surge Chamber in figure C.2. The figures are numerical stable when using  $dt = 0.1$ , and the maximum and minimum values differs insignificantly. The oscillation in the Surge Headbay is slower than in the Surge Chamber.

## 5.4 Increase power output

A calculation model for investigating a potential increase in power output of the existing turbines is presented here. The parameters  $n$ ,  $D_1$ ,  $D_2$   $NPSH_A$

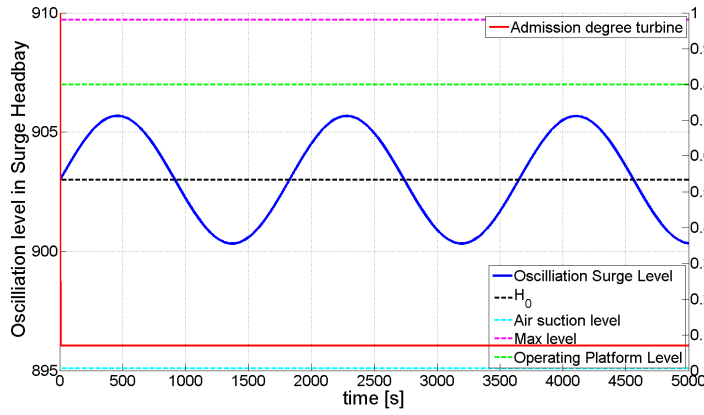


Figure 5.4: Verification Surge Headbay load rejection

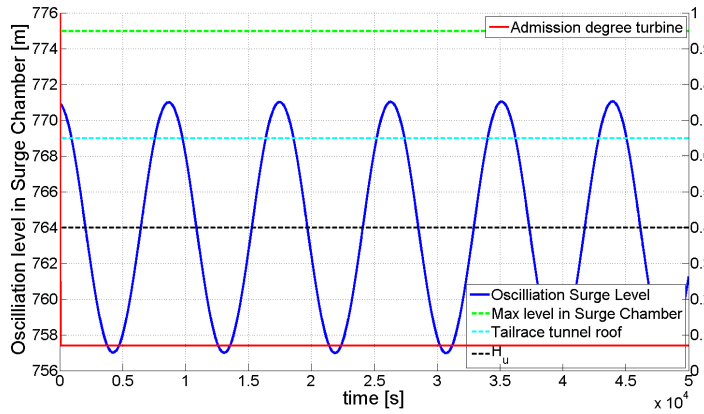


Figure 5.5: Verification Surge Chamber load rejection

and  $H_n$  are known. The calculation model starts by using the cavitation limit as a design criteria, and a safety factor of 15% is subtracted yielding the relationship (5.22).

$$NPSH_T \leq NPSH_A(1 - 0.15) \quad (5.22)$$

Equation (2.14) for calculating  $NPSH_T$  is rearranged in order to find  $\beta_2$  directly in equation (5.25). This correlation is found by using the reduced value of  $\underline{u}_2$  (5.23) and the relationship in (5.24).

$$\underline{u}_2 = \frac{u_2}{\sqrt{2gH_n}} \quad (5.23)$$

At nominal load does the absolute meridian velocity increase, while the outlet angle  $\beta_2$  remains the same. Equation (5.24) yields the correlation between flow at full load and best efficiency point. The value of the admission coefficient  $\kappa$  is assumed to be 1.15 for a medium head Francis turbine.

$$\kappa = \frac{c_{m2}}{*c_{m2}} = \frac{Q_n}{*Q} \quad (5.24)$$

## 5 Increase power output

---

A selection of favourable outlet angles are found for a range of  $NPSH_T$  starting from (5.22) and decrease with an increment of 0.1m. An iterative procedure is used to find  $\beta_2$  from equation (5.25) where the value of  $b$  depends on the speed number given by equation (5.26). Outlet angles that are larger than  $20^\circ$ , or smaller than  $13^\circ$  are discarded.

$$\beta_2 = \tan^{-1} \left( \sqrt{\frac{1}{a\kappa^2} \left( \frac{NPSH_T}{H_n \bar{u}_2^2} - b \right)} \right) \quad (5.25)$$

$$^* \Omega = \bar{u}_2^{3/2} \sqrt{\pi \tan(\beta_2)} \quad (5.26)$$

In order to verify that the figures are calculated at BEP the values of  $^* c_{m2}$  and  $^* c_{u2}$  are calculated according to equations (5.27) and (5.28). Where  $^* c_{u2} = 0$  at BEP.

$$^* c_{m2} = u_2 \tan(\beta_2) \quad (5.27)$$

$$^* c_{u2} = u_2 - \frac{^* c_{m2}}{\tan(\beta_2)} = 0 \quad (5.28)$$

The volume flow  $^* Q$  is calculated using equation (5.29). An increase in the volume flow compared to the existing is expected.

$$^* Q = \left( \frac{^* \Omega (2gH_n)^{3/4}}{\omega} \right)^2 \quad (5.29)$$

$NPSH_T$  is recalculated according to (2.14) to ensure that the cavitation criteria is fulfilled at nominal load. Thereafter, the power output is calculated according to the power equation (5.32) for hydraulic efficiency in the range from 0.92 to 0.96.  $H_{new}$  is the reduction in net head  $H_e$ , which is accounted for by first calculating the head losses in the water way according to equation 5.30 and the new head is calculated according to equation 5.31. A matlab program is developed in order to present the correlation between the reduction in net head and the power output. The program is presented in appendix B.3.

$$h_f = c_1 Q_{station}^2 + c_2 Q_{unit}^2 + c_t Q_{unit}^2; \quad (5.30)$$

$$H_{new} = H_0 - h_f \frac{Q_{new}^2}{Q_{unit}^2} \quad (5.31)$$

$h_f$  - Total headloss from intake to exit of draft tube [m]

$Q_{station}$  - Total volume flow in the station [m<sup>3</sup>/s]

$Q_{unit}$  - Volume flow one unit [m<sup>3</sup>/s]

$Q_{new}$  - New volume flow for one unit [m<sup>3</sup>/s]

$$P_n = \eta \rho g Q_{unit} H_{new} \quad (5.32)$$

An investigation of drawing "MB9-043.1109 A; Runner" has lead to the conclusion that it is possible to increase the outlet diameter by maximum 60 mm. This comprises a change of lower cover and draft tube cone.

## Chapter 6

---

# Results

---

The objective of the simulation of the dynamic response in the water way is to find out if the system can handle an increase in volume flow. The result is then used in the investigation of potential increase in power output.

### 6.1 Analysis: Existing Hydraulic Conditions

The full analysis of the existing hydraulic conditions is described in appendix C.2, and a summary is presented in the following. Only worst case scenarios are considered.

#### 6.1.1 Oscillation in Surge Headbay

Table 6.1 presents the maximum up- and downsurge in the Surge Headbay with 4 units in operation. All surge levels was within the limits. The maximum upsurge  $Z_{max}$  was 909.3 masl at highest flood level (HFL) in the intake illustrated in figure C.3. In table 6.2 the minimum levels in the intake for operation of 1 to 4 units presented.

For the minimum draw-down water level (MRWL) of 895.2 masl in the intake was it found that only one unit can be operated. In all these simulations the upsurge in the Surge Chamber did not exceed the limit of 775 masl, nor did the downsurge go below 764.7 masl.

Scenario	$Z_{max}$ , [masl]	$Z_{min}$ , [masl]	Figure
HFL	909.3	898.8	C.3

Table 6.1: Results: analysis of existing conditions in Surge Headbay 4 units

No of units	$H_0$ , [masl]	Figure
1	895.2	C.4
2	896.4	C.5
3	897	C.6
4	897.4	C.7

Table 6.2: Results: Analysis of existing conditions at MRWL levels

### 6.1.2 Oscillation in Surge Chamber

For 1 to 4 units in operation the maximum levels in the tailrace are presented in table 6.3. The simulations clearly showed that reload/reject sequences must be carried out carefully in order to avoid excessive surges. All other tailrace levels in table 4.6 lead to surges that are well within the limits of the chamber. In the graphs are the upsurges sudden because the oscillation alters between a free-water surface with a large area in the tunnel. When the water level rise above the tailrace tunnelroof denoted by the turquoise dotted line, a sudden area contraction occurs. The graphs presents worst case scenarios with a high water level in the tailrace, which is not normally the case.

No of units	$H_u$ , [masl]	Figure
4	768	C.8
3	768.3	C.9
2	768.7	C.10
1	769.2	C.11

Table 6.3: Results: Analysis of existing conditions in Surge Chamber

### 6.1.3 Pressure in front of turbine

The pressure in front of the turbine is determined by the highest water level in the Surge Headbay and with the volume flow of one turbine  $71 \text{ m}^3/\text{s}$ . The result is shown in figure 6.1, and the maximum water pressure in front of one turbine is 172.4 mWC. The pressure rise is governed by the elevation in the Surge Headbay until the valve closes. Thereafter does the oscillation of the water hammer govern the pressure with a period of 0.66s.

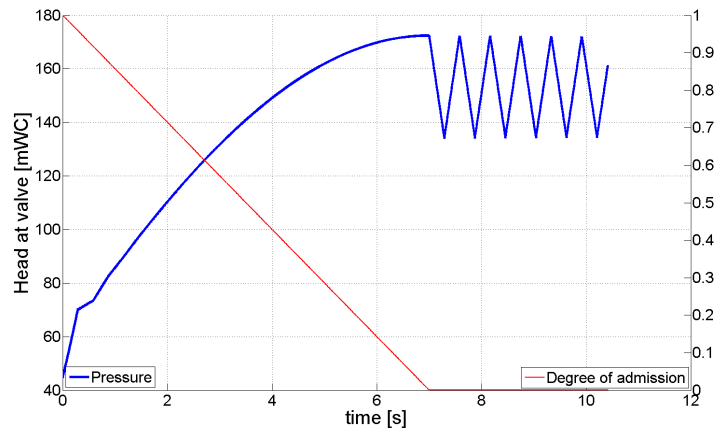


Figure 6.1: Pressure in front of turbine,  $Z_{max} = 909.3 \text{ masl}$  and  $Q_{unit} = 71 \text{ m}^3/\text{s}$



## 6.2 Analysis: Increasing Volume Flow

The analysis aims to find the maximum increase in volume flow, which does not compromise the safety of the plant. Only the worst case scenarios are evaluated.

### 6.2.1 Oscillation in Surge Headbay

It is found that an increase in nominal volume flow of the station to  $340\text{m}^3/\text{s}$  is possible. The upsurge in the Surge Headbay reaches a level of  $909.7\text{ masl}$ , and a reload/reject sequence does not lead to a higher level as can be seen in figure 6.2.

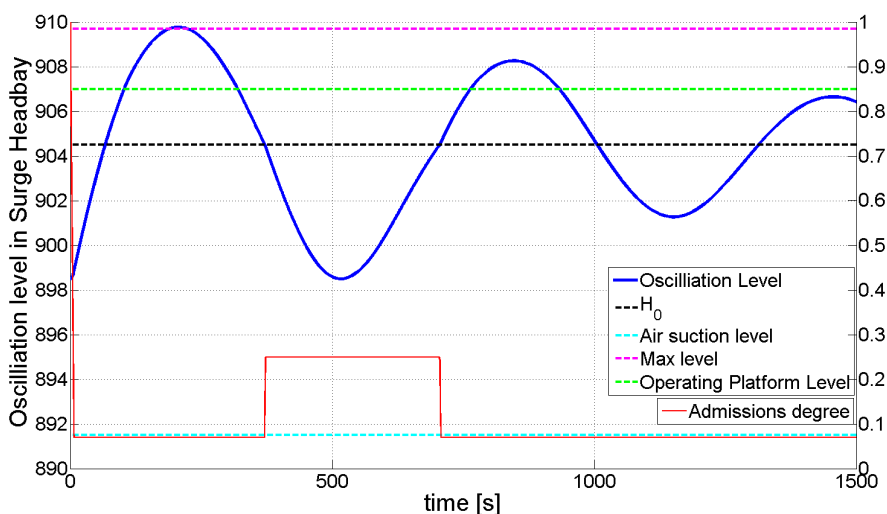


Figure 6.2: Surge oscillation SH,  $H_0 = 904.5\text{ masl}$   $Q_{n,station} = 340\text{m}^3/\text{s}$

The minimum draw-down level must be increased for the new volume flow. For operation of 1 – 4 units are they presented in table 6.4. The result of 4 units in operation is illustrated in figure 6.3, all other figures can be found in appendix C.3.

No. of units	MRWL [masl]	Increase, [m]	Figure
1	896	0.8	C.14
2	897	0.6	C.13
3	897.5	0.5	C.12
4	897.8	0.4	6.3

Table 6.4: MRWL levels for increased volume flow

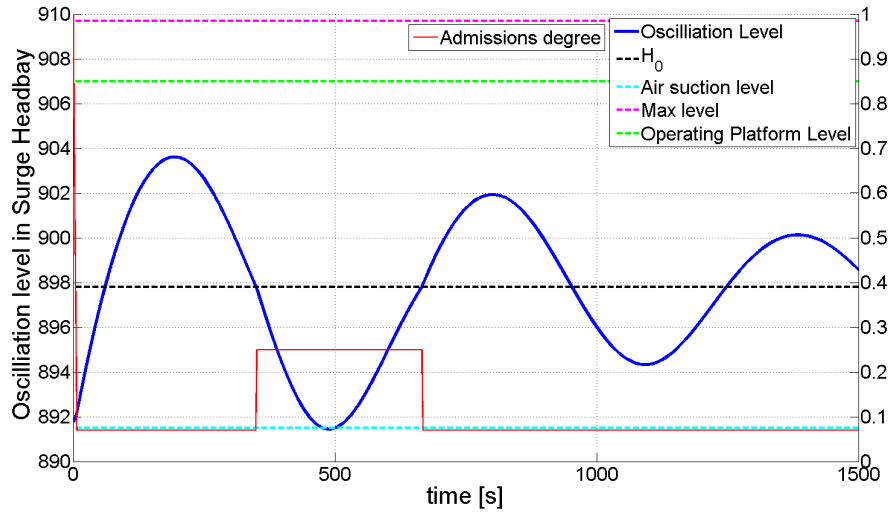


Figure 6.3: Surge oscillation in SC,  $H_0 = 897.8$  masl and  $Q_{n,station} = 340\text{m}^3/\text{s}$

### 6.2.2 Oscillation in Surge Chamber

No of units	$H_u$ [masl]	Decrease [m]	Figure
4	767.6	0.4	6.4
3	767.9	0.4	C.15
2	768.2	0.5	C.16
1	769.2	0	C.17

Table 6.5: Maximum levels in tailrace with increased volume flow

The increased volume of  $85\text{m}^3/\text{s}$  for one unit also influences the maximum level in the tailrace. The identified levels are presented in table 6.5. Figure 6.4 illustrates the result for 4 units in operation, all other figures can be found in appendix C.3. The oscillation has characteristic peaks due to a sudden area contraction when the water rises above the tunnel roof.

### 6.2.3 Pressure in front of turbine

The result of pressure calculations with an increased flow rate of  $85\text{ m}^3/\text{s}$  for one unit with  $H_0 = 909.7$  masl is shown in figure 6.5. The closing time is 7 seconds and the maximum pressure is 177 mWC.

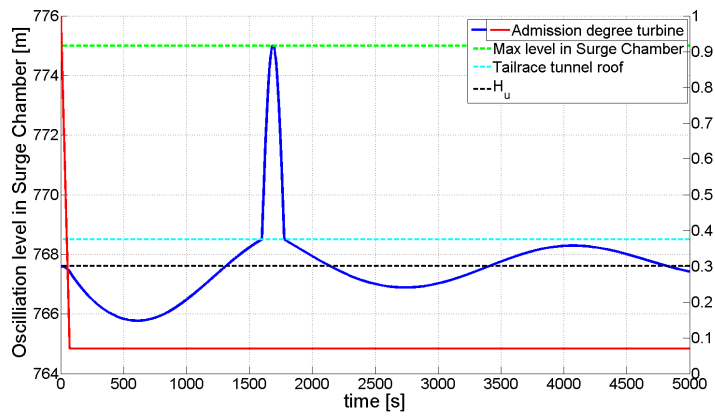


Figure 6.4: Surge oscillation in SC,  $Q_{n,station} = 340\text{m}^3/\text{s}$ ,  $H_u = 767.6$  masl

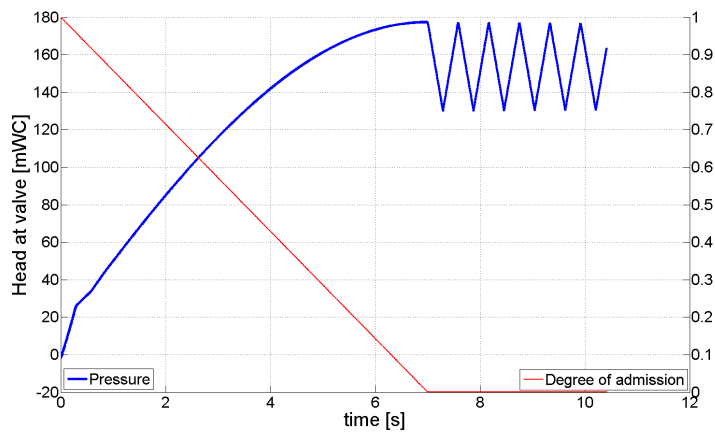


Figure 6.5: Pressure in front of turbine,  $Z_{max} = 909.7$  masl  $Q_{unit} = 85\text{m}^3/\text{s}$

### 6.3 Analysis: Increasing Power Output

It is concluded from the analysis of increasing power output that an increase of nominal volume flow for one unit is possible up to  $Q_{n,unit} = 85\text{m}^3/\text{s}$ . The calculation method developed in this thesis is presented in section 5.4. Table 6.6 presents the maximum percentile increase in nominal power output for one turbine, which is compared to the existing  $P_n = 82\text{ MW}$ . Dia00 refers to the existing outlet diameter, Dia06 to an increased diameter of 60 mm when the method presented in section 5.4 is used. The Sintef method presented in section 3.1.3 is altered by starting with assuming a power output that yields a volume flow of  $85\text{ m}^3/\text{s}$ , which is within the cavitation limit. In the table Sintef00 refers to the existing diameter and Sintef03 to the increased. The cavitation limit in these cases is not exceeded. All calculated values can be found in appendix D. It is calculated for a range of turbine efficiencies from 0.93 to 0.95 at nominal load. None of the volume flows exceeds the limit of  $85\text{ m}^3/\text{s}$ , and the outlet angles are within normal range. The differences in presented net head are due to different calculated volume flows.

	<b>Dia00</b>		<b>Dia06</b>		<b>Sintef00</b>		<b>Sintef06</b>	
<b>Efficiency</b>	$H_e$ [m]	%	$H_e$ [m]	%	$H_e$ [m]	%	$H_e$ [m]	%
0.93	123.3	14	122	15	121.9	13	121.9	16
0.94	123.3	15	122	16	121.9	14	121.9	17
0.95	123.3	16	122	17	121.9	15	121.9	18

Table 6.6: Maximum percentile increase in nominal power output for one unit

The reduction in head due to increased volume flow is accounted for and illustrated by the blue line in figure 6.6. The figure presents the result of one turbine when four units are in operation. The pink, green and red line represent increase in power output as a function of volume flow and net head for the used turbine efficiencies. The dotted black line represents the maximum allowable volume flow  $85\text{ m}^3/\text{s}$ . The circles are the calculated values for Dia00. For a turbine efficiency of 0.93 does the power output almost coincide with the reduced head line.

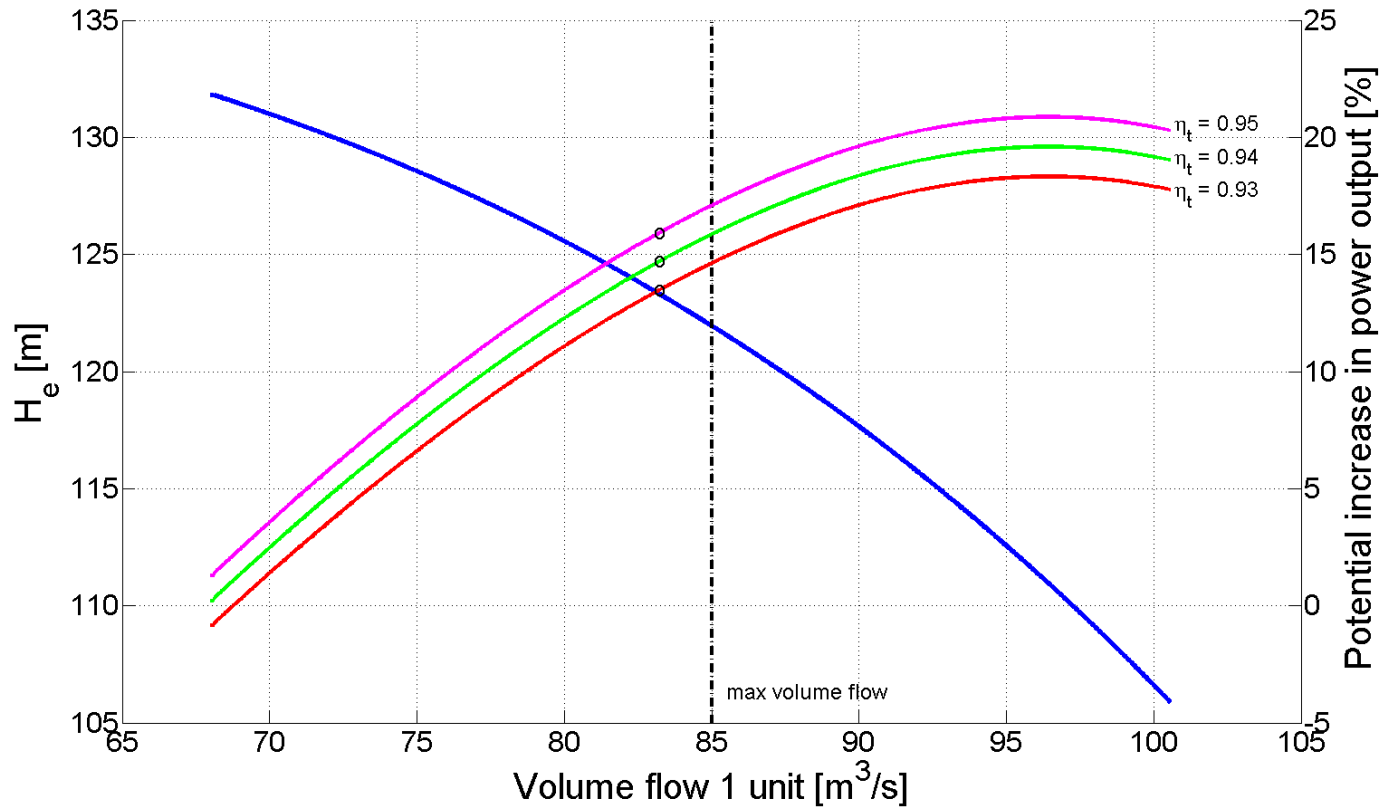


Figure 6.6: Percentile increase in power output as a function of volume flow and reduction in net head. For 1 turbine when 4 are in operation.



## Chapter 7

---

# Discussion

---

In order to prepare a final conclusion is the purpose of this chapter to evaluate the results presented in 6.

### 7.1 Hydraulic considerations

The results show that the design of the Surge Headbay effectively damps down the oscillation. In the investigation of the existing hydraulic conditions did first upsurge yields the maximum level of 909.3 masl. Additional reload/reject sequense did not rise above this level, and therefore does the sequence only consist of one turbine one time. The surge rises above the platform level, but this is not considered to be a problem as long as there are not stored any equipment that may be destroyed there. The area cross-sectional area in the Surge Chamber is measured, and it is probably larger. The sudden upsurges may therefore be as severe as they seem. The sudden upsurge is due to a transition between free water surface conditions in the tunnel to the smaller cross-sectional area. In the Matlab program an Euler code which is used which is not the most accurate numerical method. This program is based on a simplified waterway system, and all variables are not accounted for. Due to all reasons mentioned above it is highly probable that the oscillations in the chambers are over estimated. It is assumed that this also applies to the water hammer calculations.

It is clear from the analysis of existing hydraulic conditions that the highest regulated water level imposes the largest constraint on increasing volume flow. All other critical levels impose a constraint on the regulation of the plant. The minimum draw-down level depends on the number of turbines in operation, and a larger volume flow increases the levels. On the contrary to the maximum tailrace levels, which decreases. The used headloss coefficients are obtained from site tests at Ruacana. For the surge calculation could it have been of interest to include the governor equations. The pressure in front of the turbines is not of concern for increased volume flow. If it had been a problem could the closing time of the turbine be increased, and the pressure is reduced.

### 7.2 Power output

The submergence of the system is not a restrictive factor and therefore it yields a clear improvement potential. The available information about the design of the existing runners is not sufficient to establish a complete picture. It is unfortunately impossible to establish characteristics as flow angles ect. A new runner is likely to avoid the cavitation problem by increasing the inlet angles and alter the blade lean angle. Large changes in inlet and outlet angles can be compensated for by replacing the guide vanes.

It is calculated for a range of turbine efficiencies from 0.93 to 0.95 at nominal load, because without further analysis of a potential new runner design it is impossible to determine an accurate value. The efficiency of a new runner implemented into an existing turbine structure is lower than for a new turbine. It has been considered feasible to use a turbine efficiency of 0.93. Information about the efficiency of other components of the turbine are not known, and are therefore not included.

The calculation method developed in this thesis finds the potential increase in volume flow from the submergence of the system, and thereafter estimates the nominal power output. This is the main difference from the Sintef method, where increase in nominal power output is assumed at the beginning. The overall result in the Sintef method claims an increase in power output of 20% when the reduction in head is not accounted for.

The estimated values of potential nominal power output differs for the two methods. In the case of keeping the existing diameter does the method from this thesis predict an increase of 14% with an turbine efficiency of 0.93. The Sintef method estimates an increase of 16%. These calculations have not included all variables and assumes a new runner design with an increased volume flow capacity. A new nominal volume flow of 85 m<sup>3</sup>/s is 25% larger than the existing. The percentile increase is very large and probably unobtainable. An increase in volume flow of 16% is more conservative and yields a nominal power output increase of 10%, with a turbine efficiency of 0.93 and the net head is 126 m. The new unit under installation is designed for a head range determined by the existing conditions. A large increase in volume flow could also affect the design conditions for this turbine, and probably lead to a different head range.

Both calculations are in agreement that it is more to gain by increasing the diameter. In this case must the upper part of the draft tube cone and lower cover be replaced in addition to the runner. The increase in diameter is not large and therefore it is not necessary to replace wicket gates and spiral casing. For the Sintef method is the percentile increase in power output 18% and the method developed here predicts 15%. The question about economic viability arise since the increase is small. Both estimates are probably to high.



## Chapter 8

---

# Conclusion

---

This thesis aims to estimate a potential increase in nominal power output at Ruacana by only replacing the runner. The existing turbines have been reviewed to the extent it is possible, and it is concluded that there exists an improvement potential.

The power output can be improved either by increasing the volume flow and/or enhancing efficiency. The existing hydraulic conditions have been evaluated, and an investigation concluded that a maximal increase in the nominal volume flow to  $Q_{n,unit} = 85\text{m}^3/\text{s}$  is possible. It is found that this is within the restrictions of surge oscillation and pressure in front of the turbines. The minimum-draw down level in the Surge Headbay must be increased and depends on the number of turbines in operation. This also yields for the highest level in the tailrace which has to be decreased. An increase in efficiency can be expected with a new runner.

It is concluded that it can be possible to increase the nominal power output from 10 – 14%. Assuming a turbine efficiency of 0.93 and a replacing the runner with higher volume flow capacity.



## Chapter 9

---

# Further Work

---

The objective of this thesis was to investigate the possibility of increasing power output. All aspects of a rehabilitation project have not been evaluated. Some examples of additional inquiries are presented here.

Further design of a Francis turbine that can be appropriate for all existing constraints is necessary. It should be followed by an optimization process using computational fluid dynamics. Other parts of the turbine could be investigated in more depth. Review the guide vanes and wicket gate conditions for increased volume flow. A new design of the runner may lead to altered inlet angles that are not in correspondence to the guide vanes. Further inspection of the flow conditions of the existing guide vanes is necessary.

Here, only the technical aspects has been evaluated as mentioned earlier. A financial analysis can be performed, because the realization of a rehabilitation projects is highly dependent on the economic viability. The calculation method developed in the thesis is not verified and should be verified.

Other hydrological aspects can be evaluated, such as the river flow. Is it enough water throughout the year that it is favourable to increase the volume flow? A review of the regulation scheme at Ruacana can also be performed.



---

# Bibliography

---

- [1] 21st African Hydro Symposium. Proceedings. Namibia, 2009.
- [2] Vöest Alpine. Mechanical drawings. Recieved from NamPower, 1973.
- [3] G. V. Aronovich, N. A. Kartvelishvili, and Ya. K Lyubimtsev. *Water Hammer and Surge Tanks*. Keter Press, 1970.
- [4] J. E. Borges. A three-dimensional inverse method for turbomachinery: Part 1 - theory. *Journal of Turbomachinery*, 112, 1990.
- [5] H. Brekke. Hydraulic design strategy for Francis turbines. *Hydropower & Dams*, 1996.
- [6] H. Brekke. State of the art in turbine design. *IAHR congress Beijing, Conference Proceedings*, 2001.
- [7] H. Brekke. *Pumper og Turbiner*. NTNU, Vannkraftlaboratoriet, 2003.
- [8] N. Caron and F. Arzola. Performance measurments on refurbished turbines of 770,000kw at Guri hydroelectric complex. *5<sup>th</sup> IGHEM Ineternational Conference, Luceren - Switzerland*, 2004.
- [9] CEDREN. International seminar on environmental effects of hydropeak-ing. Trondheim, Norway, March 2009.
- [10] Water Power & Dam Construction. *Yearbook*. Wilmington Media Ltd, 2006.
- [11] Water Power & Dam Construction. *Yearbook*. Wilmington Media Ltd, 2009.
- [12] O. G. Dahlhaug. Personal conversation.
- [13] F. de Siervo and F. de Leva. Modern trends in selecting and designing Francis turbines. *Water Power & Dam Construction*, pages 28 – 35, August 1976.
- [14] N. Désy, A Demers, and A. Nichtawitz. Experience with large Francis rehabilitation projects. *Hydropower & Dams, Hydro 2009 conference Lyon*, 2009.
- [15] A. Espag. Personal conversation.

- [16] R.E Featherstone and Nalluri C. *Civil Engineers Hydraulics*. BSP Professional Books, 1988.
- [17] E. Göde. Performance upgrading of hydraulic machinery with the help of CFD. *Notes on Numerical Fluid Mechanics and Multidisciplinary Design*, 100:299–310, 2009.
- [18] Paula Hardy and Matthew D. Firestone. *Lonely Planet: Botswana & Namibia*. 2007.
- [19] Andritz Hydro. Hydro news. Customer magazine, - 2009.
- [20] Voith Hydro. Hypower. Company brochure, - 2009.
- [21] H. Jernsletten and H. Brekke. Beregning av effektøkningspotensial i norske kraftverk. Sintef Energiforskning, 1996.
- [22] African Business Journal. Nampower. <http://www.tradersafrica.com/index.asp>, February – May 2002.
- [23] A. Kimani and Skuncke O. Upgrading of Kiambere hydroelectric plant in kenya. *Hydropower & Dams, Hydro 2009 conference Lyon*, 2009.
- [24] E. Kleinhansen. Personal conversation.
- [25] G Muller. Expanding Ruacana powerstation. 21st Africa Hydro Symposium.
- [26] NamPower. <http://www.nampower.com.na/index.asp>.
- [27] NamPower. Ruacana. Information pamphlet, 1978.
- [28] A. Nichtawitz and C. Angerer. Box canyon p.s and cabinet gorge p.s. typical issues at upgrading of turbines. *Hydropower & Dams, Hydro 2009 conference Lyon*, 2009.
- [29] Torbjørn Nielsen. *Dynamisk Dimensjonering av Vannkraftverk*. Hydro Power Laboratory.
- [30] H. W. Oh and E. S. Yoon. Application of computational fluid dynamics to performance analysis of a Francis hydraulic turbine. *Proceedings of the Institution of Mechanical Engineers, Part A: Journal of Power and Energy*, 2007.
- [31] E. V. R. Ramón, J. L. Ribalta, C. A. Tellería, and R. T. Martínez. Large Francis upgrade in Spain. successful history of collaboration. *Hydropower & Dams, Hydro 2009 conference Lyon*, 2009.
- [32] M. Sallaberger, Ch. Michaud, H. Born, St. Winkler, and M. Peron. Design and manufacturing of Francis runners for rehabilitation projects. [http://www.andritz.com/hydro-media-media-center-francis\\_runners\\_e.pdf](http://www.andritz.com/hydro-media-media-center-francis_runners_e.pdf).
- [33] P. Swiderski and J. Martin. High power Francis runner – upgrade with a new design runner. *Norcan Hydraulic Turbine Inc. report*, 1999.

- [34] R.K. Turton. *Principles of Turbomachinery*. Chapman & Hall, 1995.
- [35] E. J. Wiborg. Correspondance.
- [36] J. WU, K. Shimmei, K. Tani, K. Niikura, and J. Sato. CFD-based design optimization for hyrdo turbines. *Journal of Fluids Engineering*, 129, 2007.
- [37] E. B. Wylie and V. L. Streeter. *Fluid Transients in Systems*. Prentice-Hall Inc, 1993.





## Appendix A

---

# Ruacana Hydro Power Plant

---

Namibia holds the oldest desert in the world and is the driest country south of Sahara. It borders Angola and Zambia in the north, Botswana in the east and South Africa in the south. The country is mostly renowned for its stark and arid landscape constituting the great dunes of the Namib Desert, and the famous scorched dunes of the Skeleton Coast. This is in stark contrast to the well-watered paradise of the northern Caprivi and Kavango regions [18], which is the location of the Ruacana falls home to the Ruacana Hydro Power Plant.



Figure A.1: Ruacana Falls

When the construction of the plant started, the country was known as South West Africa and the electricity company was named the South West African Water and Electricity Corporation (SWAWEK) [26]. The country changed officially its name to Namibia in 1968, but did not become independent from South Africa until 1990. In 1996 the company changed its name and became NamPower [26].

The energy situation in Namibia is today strained , and the country experiences more and more shortages of power . The average national load has increased beyond 320 MW, which is higher than the 240 MW generated at Rucana. The country has joined the Southern African Power Pool (SAPP) in order to import energy, which constutes mainly of large coal fired power stations. In other words, the accessibility to peak power is not high enough.

There are many projects that has been investigated and planned, but the building has usually been stopped due to political reasons. One example is the 360MW Epupa Falls which also is connected to the Kunene river. Political differences with Angola has stopped the building of this [26]. In May 2006, NamPower initiated an energy awareness campaign.

## A.1 History

The construction of Ruacana experienced some political difficulties because the river Kunene flows through Angola and Namibia. Therefore, any development utilising the resource has to be agreed upon by both countries' governments. The original Ruacana scheme was negotiated with the Portuguese Authorities and reached its conclusion in 1969 [22], and consist of the following components in the Kunene River:

A large storage dam of 2600 million cubic metres is situated about 240 km upstream from Ruacana. It is designed for regulating the flood water by storing this water during the rainy season and augment the flow in the drier months. This results in a more or less steady generation of electricity at Ruacana, and a considerable source of food for Angola. The dam was completed and commissioned in 1975. Another storage dam at Calueque at about 65 km away from Ruacana is also used as a regulation dam. It includes a pumping station for supplying the Owamboland with water during the dry seasons for human and animal consumption.

To be able to sufficiently divert the water across the border into the power station in South West Africa it was necessary to build a diversion weir 1.5 km upstream of Ruacana. This was completed in January 1978. However, the Angolan Authorities would not allow closing of the diversion weir's sluice gates.

The hydro power station is built on Namibian territory with a Surge Headbay on the surface and the rest of the station lies about 140 m below. It consists of four waterways, but only three vertical shaft Francis units was installed originally and completed January 1978. A fourth unit is currently under production [27]. Further description of the waterways, runner etc is found in chapter 4. The last component was the building of a 570 km long transmission line to a distribution station near Omaruru.

All the above components including housing for personnel at Ruacana brought the total cost up to 162 millions of South African Rands (ZAR) which converts to about 113 millions Norwegian Kroners (NOK) at todays exchange rates [26].

## Appendix B

---

# Matlab Programs

---

In this appendix presents only some pages of the developed Matlab programs for water hammer and surge oscillation calculations. The code for generating graphs is left out. The entire programs can be found in the electronic attachment. The program for generating the cross-sectional area in the Surge Headbay can be found entirely in the electronic attachment.

### B.1 Water hammer Program

```
clear all
clc
tic
disp('calculating');

%----- PARAMETERS -----

Hv = 756.2;           % Elevation of turbine, reference
g  = 9.781 ;         % Gravity [m/s^2]

% Penstock
tunnel.L = 180 ;
tunnel.D = 3.6 ;
tunnel.A = (pi/4)*tunnel.D^2;
tunnel.np = 4;
tunnel.c = 0.000615;

%-----READING CROSSECTION AREA FOR SURGE HEADBAY MATRIX-----

A_surgelevel = dlmread('crossection.xls');

%-----

L = tunnel.L;

a  = 1200;
dx = 5;
dt = dx/a;
```

```

x0 = dx;
Q0 = 85;
tmax = 2500;
x = x0;
l = 1;
y = 1;
Qn = Q0;

Z(1) = 909.3;           % Maximum surge level in SH.
B = a/(g*tunnel.A);
R = tunnel.c;

Tl= round(7/dt);      % Closing time turbine
k = (1-1e-7)/Tl;
%-----

for t = 1:1:tmax

    for x = x0:dx:L    % Storing initial values at t=0
        Q(x,t) = Q0;
        H(x,t) = Z(1);

    end
end

%%
kappa = 1;

for n = 1:1:tmax
    if n < Tl
        kappa = kappa - k;
    else
        kappa = 1e-7;
    end
    K(n,1) = kappa;

    for x = x0:dx:L
        if n == 1      %Initial values at t = 1
            Q(x,n) = Q0;
            if x == x0;
                H(x,n) = Z(1);
            else
                H(x,n) = H(x-dx,n) - R*Q(x-dx,n)*abs(Q(x-dx,n));
            end

            Hn = H(L,1);

        elseif x == x0
            z1s = round(Z(n-1)*10)/10 ;    %Round off to one decimal

            for i = 1:length(A_surgelevel)
                l = A_surgelevel(i,1);
                if l == z1s
                    y = i;
                end
            end
        end
    end
end

```

```

As = A_surgelevel(y,2);

Z(n) = Z(n-1) + dt*Q(x,n-1)/As;
H(x,n) = Z(n);
Cb = H(x+dx,n-1) + R*Q(x+dx,n-1)*abs(Q(x+dx,n-1));
Q(x,n) = (1/B)*(H(x,n) - Cb) + Q(x+dx,n-1);

elseif x>x0 && x<L
Ca = H(x-dx,n-1) - R*Q(x-dx,n-1)*abs(Q(x-dx,n-1));
Cb = H(x+dx,n-1) + R*Q(x+dx,n-1)*abs(Q(x+dx,n-1));
Qr = Q(x+dx,n-1) - Q(x-dx,n-1);
H(x,n) = 0.5*(Ca + Cb - B*Qr);
Q(x,n) = (1/B)*(H(x,n) - Cb) + Q(x+dx,n-1);

elseif x == L

Cv = (kappa*Qn)^2/Hn;
Ca = H(x-dx,n-1) + B*Q(x-dx,n-1) - ...
R*Q(x-dx,n-1)*abs(Q(x-dx,n-1));
Q(x,n) = -B*Cv*0.5 + 0.5*sqrt((B*Cv)^2 + 4*Cv*Ca);
H(x,n) = (Q(x,n)/(kappa*Qn))^2*Hn;
end
end
end
end
%%

```

## B.2 Surge Oscillation Program

```
%----- OSCILLIATION ENTIRE SYSTEM -----  
clear all  
clc  
  
tic  
disp('calculating');  
  
%----- PARAMETERES -----  
  
H_0 = 904.5; % Normal water level in diversion weir  
g = 9.781 ; % Gravity [m/s^2]  
c_s = 0.00001; % Assumed value  
  
%Pressure tunnel 1.1  
L_t1 = 1215 ; % Length [m]  
D_t1 = 8.3 ; % Diameter [m]  
A_t1 = (pi/4)*D_t1^2 ; % Area [m^2]  
  
%Pressure tunnel 1.2  
L_t2 = 285 ; % Length [m]  
D_t2 = 7.4 ; % Diameter [m]  
A_t2 = (pi/4)*D_t2^2 ; % Area [m^2]  
  
%Average pressure tunnel 1  
L_1 = L_t1 + L_t2 ; % Length [m]  
A_1 = (L_t1*A_t1 + L_t2*A_t2)/(L_t1+L_t2); % Area [m^2]  
c_1 = 5.2e-5 ; % Headloss coefficient  
  
% Penstock, tunnel 2  
L_2 = 182.1 ;  
D_2 = 3.6 ;  
A_2 = (pi/4)*D_2^2;  
np = 4; % Number of penstocks  
c_2 = 6.5e-4;  
  
% Surge Chamber  
  
A2_s = [765 40000; 766 40000; 767 40000; 768 40000; 769 816; 770 802; ...  
771 768; 772 850; 773 802; 774 789; 775 782 ];  
%Tailrace tunnel roof is at 769, areas below are therefore LARGE....  
%Read from drawing  
  
% Tailrace, tunnel 3  
L_3 = 675 ;  
w_3 = 11; % Width of tunnel  
h_3 = 13.9; % Height  
A_3 = w_3*h_3 ;  
H_u = 769.2; % Water level in Tailrace  
c_3 = 0.4e-4;  
  
%-----READING CROSSECTION AREA FOR SURGE HEADBAY MATRIX-----  
  
A_surgelevel = dlmread('crossection.xls');
```

```

%----- INITIAL VALUES AT t=0 s -----
Q0          = 4*71;
Q_1(1,1)    = Q0;          % Volume flow in pressure tunnel (1)
Q_2(1,1)    = Q0;          % Volume flow in penstock (2)
Q_3(1,1)    = Q0;          % Volume flow in tailrace (3)
z1(1,1)     = H_0 - c_1*Q0*abs(Q0); % Initial level in Surge Headbay
z2(1,1)     = Q0*0.003+ 762.4; % Initial level in Surge Chamber
Q_s1(1,1)   = 0;          % Volume flow into Surge Headbay
Q_s2(1,1)   = 0;          % Volume flow into Surge Chamber
Hn          = 130.2;      % Design head
Qn          = 284;        % Design flow
dt          = 0.1;        % Time step
tmax        = 5000;       % Maximum calculation time

kappa(1,1) = 1;
y =1;
l=1;
%----- Surge Oscillation -----
%%
n = 3068;    %Second interception point with stationary pressure line
o = n + 5;
p = 6659;    % Third interception point with stationary pressure line
q = p + 18;
r = 6368;
s = r + 18;
u = 6800;
v = u + 18;

for t = 2: tmax

    if t < 70          %Determines the opening degree of the turbine
        kappa(t,1) = 1 - t*0.01329;
    % elseif t < n
    %     kappa(t,1) = 0.07;
    % elseif t >= n && t < o
    %     kappa(t,1) = 0.07 + 0.01*(t-n);    %Reloading one turbine
    % elseif t >= o && t < p
    %     kappa(t,1) = 0.25;
    % elseif t >= p && t < q
    %     kappa(t,1) = 0.25 - 0.01*(t-p);
    % elseif t >= q && t < r
    %     kappa(t,1) = 0.07;
    % elseif t >= r && t < s
    %     kappa(t,1) = 0.07 + 0.01*(t-r);    %Reloading one turbine
    % elseif t >= s && t < u
    %     kappa(t,1) = 0.25;
    % elseif t >= u && t < v
    %     kappa(t,1) = 0.25 - 0.01*(t-u);
    else
        kappa(t,1) = 0.07;
    end

    z1s = round(z1(t-1,1)*10)/10 ;          %Round off to one decimal

    % Finds the crosssectional area corresponding to the surge level
    % in the Surge Headbay

    for i = 1:length(A_surgelevel)
        x = A_surgelevel(i,1);
        if x == z1s

```

```

        y = i;
    end
end

% Finds the crosssectional area corresponding to the surge level in
% the Surge Chamber

z2s(t-1,1) = round(z2(t-1,1)); %Round off to zero decimal
for j = 1:length(A2_s)
    k = A2_s(j,1);
    if k == z2s(t-1,1)
        l = j;
    end
end

As1 = A_surgelevel(y,2);
As2 = A2_s(l,2);

Q_s1(t-1,1) = Q_1(t-1,1) - Q_2(t-1,1);
Q_s2(t-1,1) = Q_2(t-1,1) - Q_3(t-1,1);

hf_1(t-1,1) = c_1*Q_1(t-1,1)*abs(Q_1(t-1,1));
hf_s1(t-1,1) = c_s*Q_s1(t-1,1)*abs(Q_s1(t-1,1));
hf_2(t-1,1) = c_2*Q_2(t-1,1)*abs(Q_2(t-1,1));
hf_s2(t-1,1) = c_s*Q_s2(t-1,1)*abs(Q_s2(t-1,1));
hf_3(t-1,1) = c_3*Q_3(t-1,1)*abs(Q_3(t-1,1));

Q_1(t,1) = Q_1(t-1,1) + (g*dt*A_1/L_1)*(H_0 - z1(t-1,1) ...
    - (hf_1(t-1,1) + hf_s1(t-1,1)));

Q_2(t,1) = Q_2(t-1,1) + (g*dt*A_2/L_2)*(z1(t-1,1) - z2(t-1,1) ...
    - Hn*(Q_2(t-1,1)/(kappa(t-1,1)*Q0)^2 - hf_2(t-1,1)));

Q_3(t,1) = Q_3(t-1,1) + (g*dt*A_3/L_3)*(z2(t-1,1) - H_u ...
    - (hf_3(t-1,1) + hf_s2(t-1,1)));

z1(t,1) = z1(t-1,1) + (dt/As1)*(Q_1(t-1,1) - Q_2(t-1,1));

z2(t,1) = z2(t-1,1) + 10*(dt/As2)*(Q_2(t-1,1) - Q_3(t-1,1));

end

```



## B.3 Reduction in head program

```
%----- Reduction in head program -----

clear all
clc

H0 = 902.7;
Hv = 764;           % Elevation of turbine, reference
Qn = 68;
Pn = 82;
tmax = 1300;
c_1 = 5.2e-5 ;     % Headloss coefficient
c_2 = 6.15e-4;
c_s = 0.00001;     % Assumed value

eta = 0.94;
rho = 997;
g = 9.781 ;       % Gravity [m/s^2]

Q2(1,1) = 68;
Q1(1,1) = Q2(1,1)*4;

hf(1,1) = c_1*Q1(1,1)^2 + c_2*Q2(1,1)^2 + 0.4e-4*Q2(1,1)^2;
k = hf(1)*Q2(1,1)^2/(Qn^2);
Hnew(1,1) = H0 - k ;
Pnew(1,1) = rho*g*Q2(1,1)*(Hnew(1,1)-Hv)*10^(-6);

for t = 2:tmax
    Q_s1(t,1) = Q1(t-1,1) - Q2(t-1,1);

    hf(t-1,1) = c_1*Q1(t-1,1)^2 + c_2*Q2(t-1,1)^2 + 0.4e-4*Q2(t-1,1)^2;
    k = hf(t-1)*Q2(t-1,1)^2/(Qn^2);
    Hnew(t,1) = H0 - k ;
    Pnew(t,1) = rho*g*Q2(t-1,1)*(Hnew(t-1,1)-Hv)*10^(-6);

    Q1(t,1) = Q1(t-1,1)+ 0.1;
    Q2(t,1) = Q1(t-1,1)/4 + 0.1;

end

Hnew = Hnew - Hv;
P93 = ((Pnew*0.93/Pn)-1)*100;
P94 = ((Pnew*0.94/Pn)-1)*100;
P95 = ((Pnew*0.95/Pn)-1)*100;
```



## Appendix C

---

# Supplement Results

---

This chapter is intended to be a supplement to the presented results. Therefore, values and description of the graphs can be found in chapter 6.

### C.1 Verification of Simulation Models

Figures C.1 and C.2 shows the oscillation for ideal conditions when reloading.

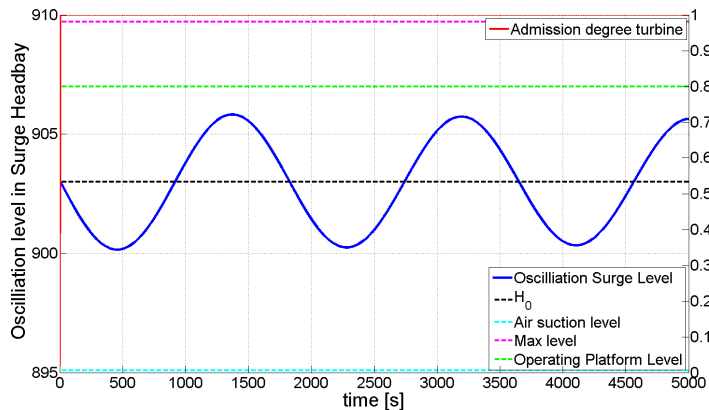


Figure C.1: Verification Surge Headbay reload

### C.2 Supplement existing hydraulic conditions

Only the critical water levels in the intake and tailrace is considered in the analysis of existing hydraulic conditions. Additional reload/reject sequences have been investigated, but only the scenarios that does not exceed the limit is presented.

#### C.2.1 Surge oscillation in Surge Headbay

The surge oscillation results are presented in the following for the worst case scenarios. All simulations include a reload/reject sequence.

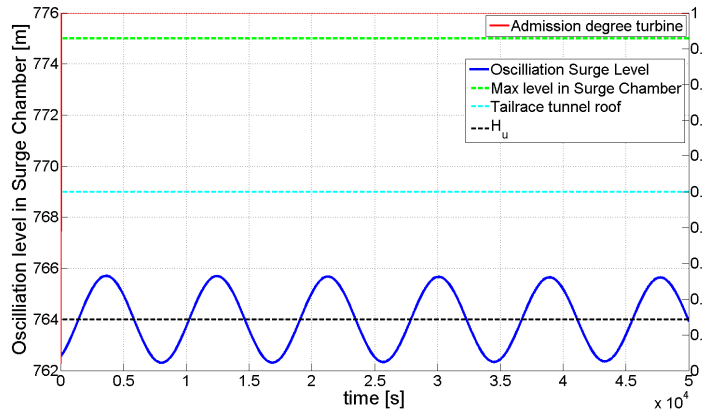


Figure C.2: Verification Surge Chamber reload

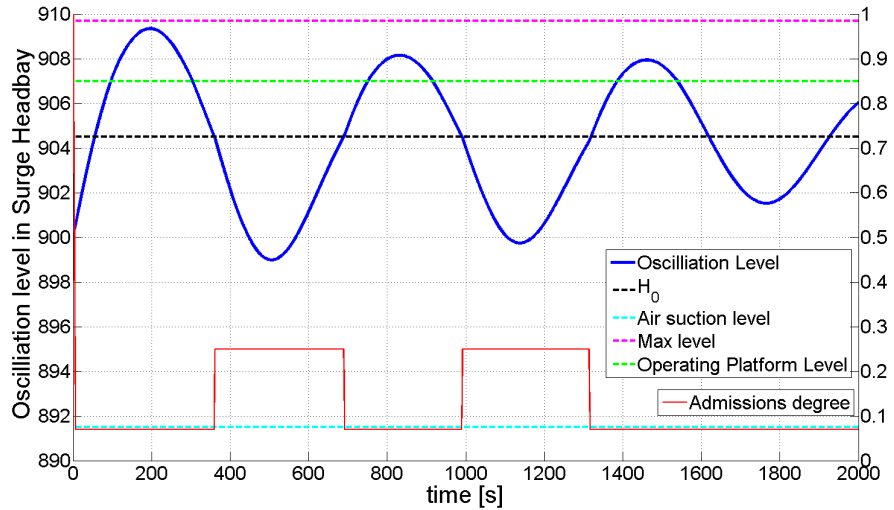


Figure C.3: Surge oscillation at highest flood level 4 units

### Highest flood level HFL

The highest flood level in the intake is 904.5 masl, and the surge oscillation is shown in figure C.3. The maximum upsurge is 909.3 masl and minimum downsurge is 899 masl. The result of the Surge Chamber is not presented here, but the load sequence yields a maximum upsurge of 774.4 masl.

### Minimum draw-down level MRWL

The minimum draw-down level in the intake is 895.2 masl, and it is found that only one turbine can operate as shown in figure C.4.

The minimum level in the intake for rejecting two units is found to be 896.5 masl. The minimum downsurge is 891.6 masl, and the maximum upsurge is 900.9 as shown in figure C.5.

In figure C.6 the lowest level in the intake is 897 masl when operating 3 units. The maximum upsurge is 901.5 masl, and the downsurge is 891.5

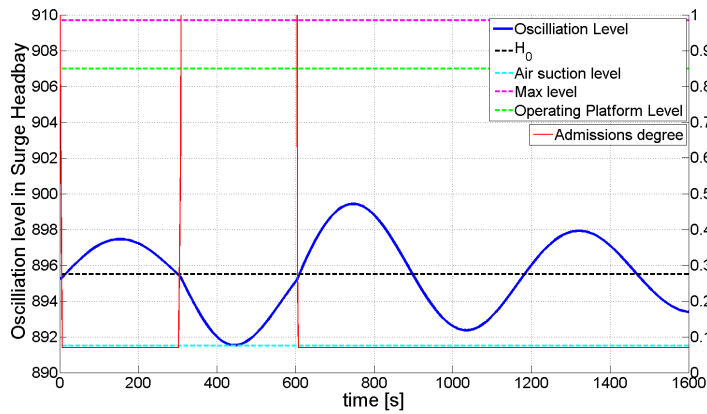


Figure C.4: Surge oscillation SH,  $H_0 = 895.2$  masl and  $Q_{unit} = 71\text{m}^3/\text{s}$

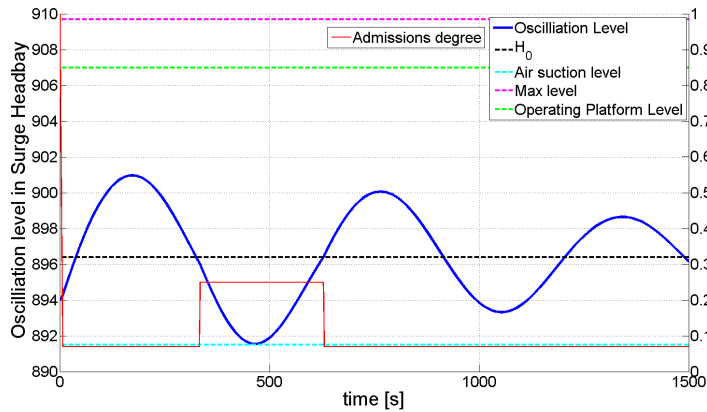


Figure C.5: Surge oscillation in SH,  $H_0 = 896.4$  masl and  $Q = 142\text{m}^3/\text{s}$

masl. The level in the intake must be 897.4 masl for operating 4 units and it is shown in figure C.7. The maximum down surge is 891.6 masl and the upsurge is 902.7 masl.

## C.2.2 Surge Chamber Results

### 4 units

The result of the investigation of the Surge Chamber shows that for a full load rejection from 4 units is only possible with a tailwater level of 768 masl as demonstrated in figure C.8. The maximum upsurge is 774.8 masl, and it shows that a reload/reject sequence at any of the upsurges will exceed the maximum limit if it is reloaded before the third upsurge.

### 3 units

The highest tailwater level is 768.3 masl when operating 3 units. A load rejection shows that the first upsurge yields the maximum of 775.1 masl. Figure C.9 shows the progression for reload/rejecting a unit at the third

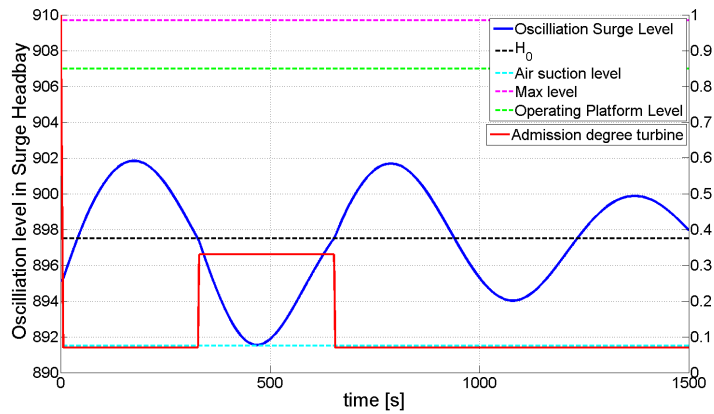


Figure C.6: Surge Oscillation in SH,  $H_0 = 897$  masl and  $Q = 213\text{m}^3/\text{s}$

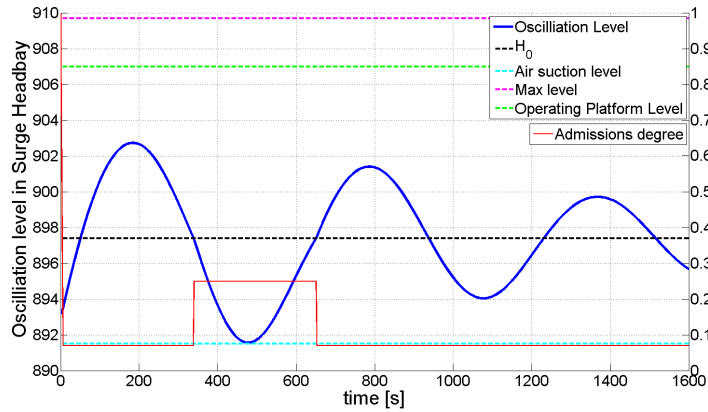


Figure C.7: Surge oscillation in SH,  $H_0 = 897.4$  masl and  $Q = 284\text{m}^3/\text{s}$

upsurge which achieved a level of 773.9 masl, which is smaller than the first upsurge.

## 2 units

For 2 units in operation can the tailwater have a level of 768.7 masl. A load rejection yields a maximum upsurge of 775, and is shown in figure C.10. A reload/reject sequence that strikes one of the upsurgings is not possible until a long time has passed.

## 1 unit

For the highest level of 769.2 masl in the Surge Chamber is it only possible to operate with one unit as the result in figure C.11 shows. The maximum upsurge level is 773.2 masl, and a reload/reject sequence that strikes one of the upsurgings at the worst possible time can not be performed until a long time has passed.

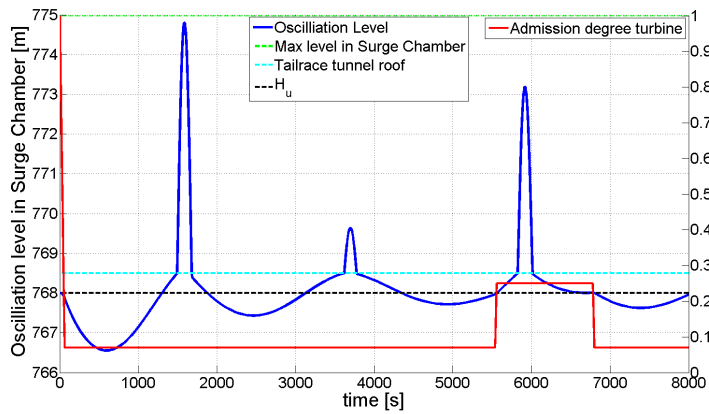


Figure C.8: Surge oscillation in SC,  $H_u = 768$  and  $Q = 284\text{m}^3/\text{s}$

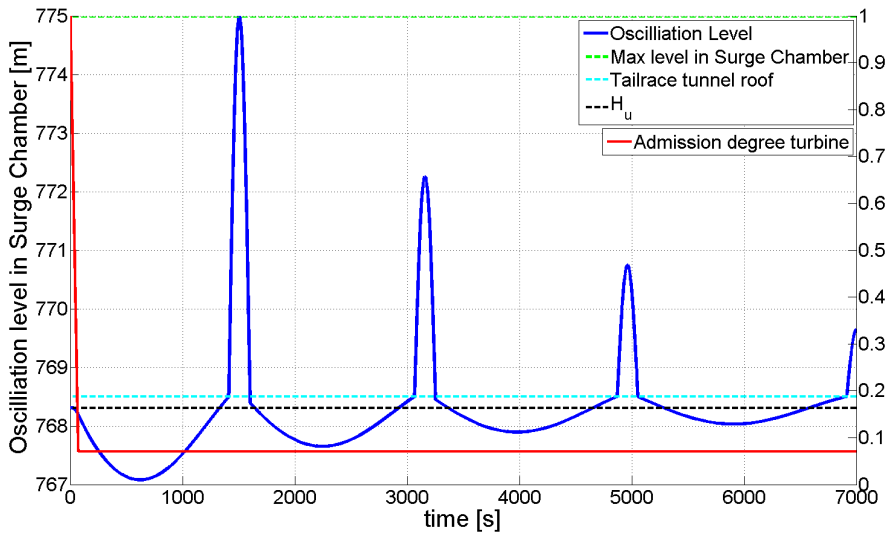


Figure C.9: Surge oscillation in SC,  $H_u = 768.3$  masl and  $Q = 213\text{m}^3/\text{s}$

### C.3 Analysis: Increasing Volume Flow extension

The results of the analysis is presented in detail in section 6.2. Here are only the graphs presented.

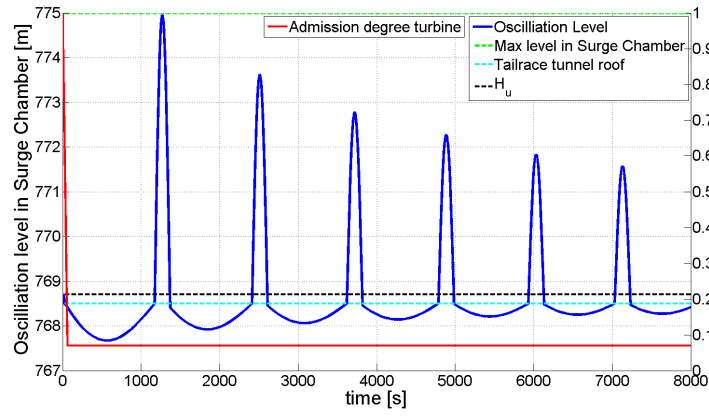


Figure C.10: Surge oscillation in SC,  $H_u = 768.7\text{masl}$  and  $Q = 142\text{m}^3/\text{s}$

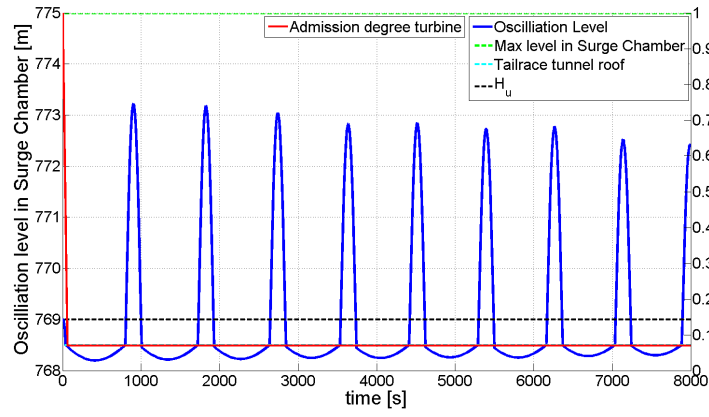


Figure C.11: Surge oscillation in SC,  $H_u = 769.2\text{masl}$  and  $Q = 71\text{m}^3/\text{s}$

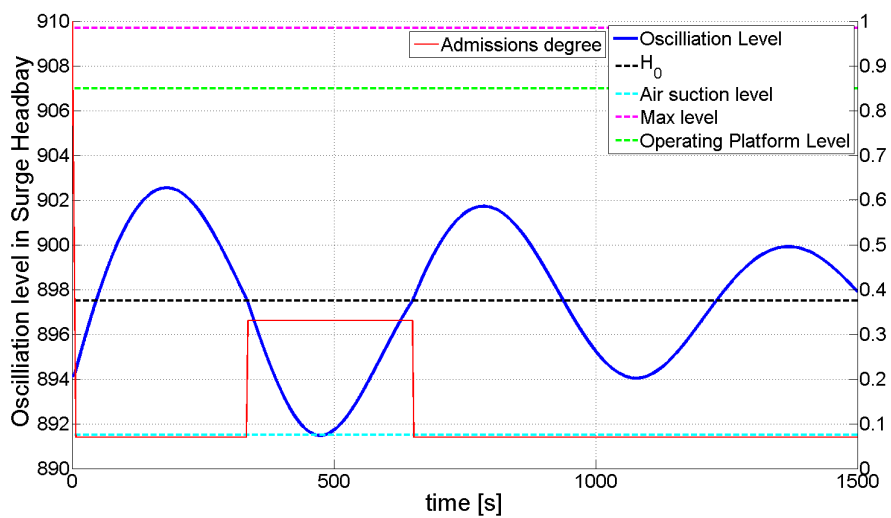


Figure C.12: Surge oscillation in SH,  $H_0 = 897.5\text{masl}$  and  $Q = 255\text{m}^3/\text{s}$



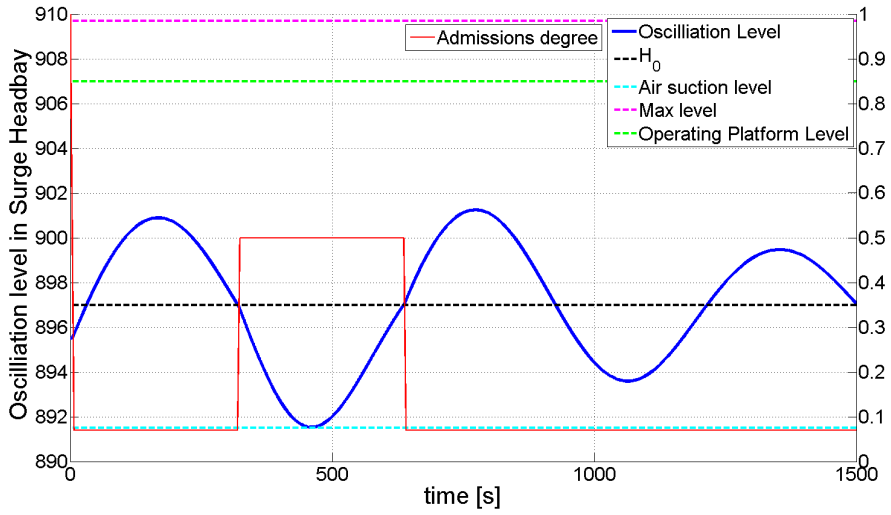


Figure C.13: Surge oscillation in SH,  $H_0 = 897$  masl  $Q = 142\text{m}^3/\text{s}$

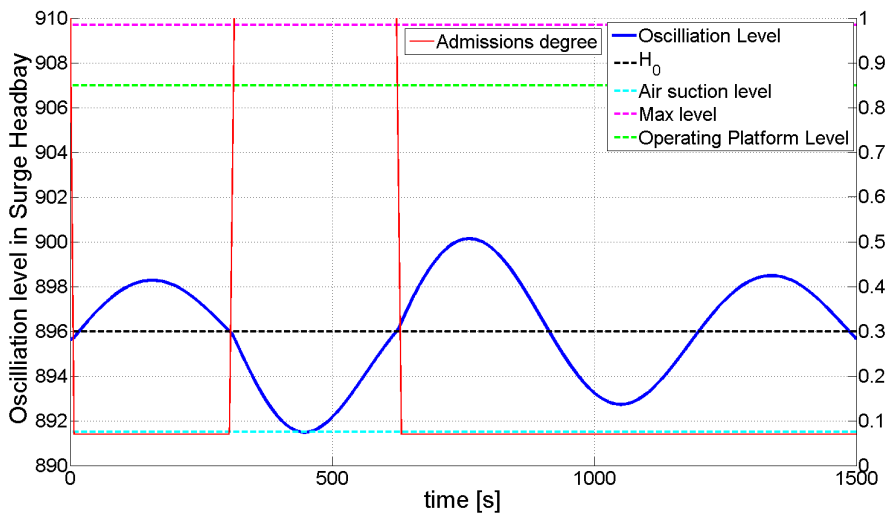


Figure C.14: Surge oscillation in SH,  $H_0 = 906$  masl  $Q = 71\text{m}^3/\text{s}$

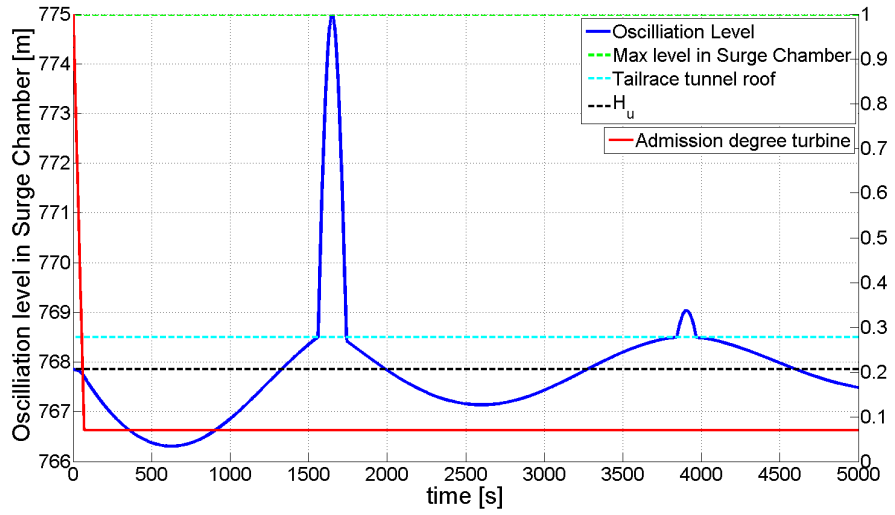


Figure C.15: Surge oscillation in SC  $H_u = 767.9$  masl and  $Q = 255\text{m}^3/\text{s}$

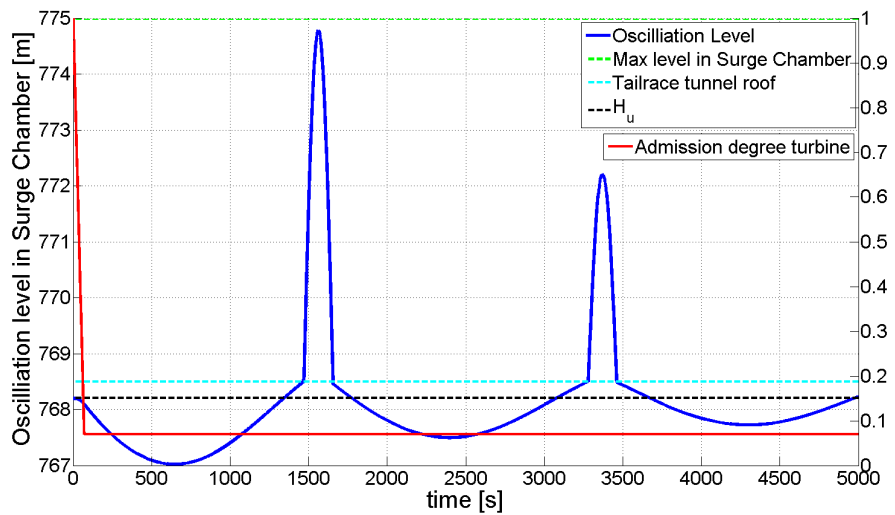


Figure C.16: Surge oscillation in SC  $H_u = 768.2$  masl and  $Q = 170\text{m}^3/\text{s}$

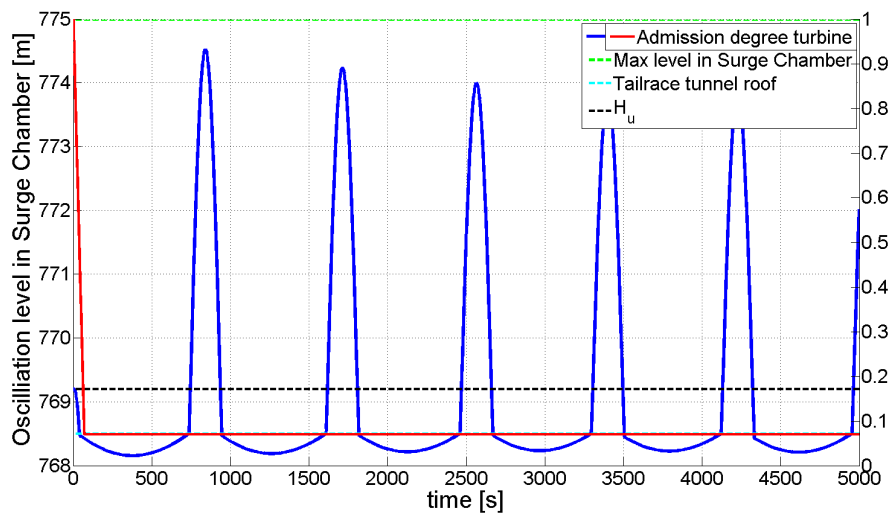


Figure C.17: Surge oscillation in SC,  $H_u = 769.2$  masl and  $Q = 85\text{m}^3/\text{s}$



## Appendix D

---

# Excel Calculations

---

D.1 Distribution of turbine types

D.2 Survey

D.3 Dia00

D.4 Dia03

D.5 Calculation of potential increase in power output  
(Sintef)

## Appendix D.1: Distribution of turbine types

Plant	Turbine type	no units	Unit Output [MW]	Diameter	Head [m]	Speed
<b>Asia</b>						
Lohair Nagpala	Pelton	4	167.5	3350	427	250
Sorang	Pelton	2	59.2	1760	673	600
Teesta Urja II	Pelton	6	233.75	3020	817	375
Chukha	Pelton	4	84	2870	463.2	300
East Toba River	Pelton	2	78.5	2210	569.88	450
Yazuihe-Yangang	Pelton	2	65.6	1650	631.75	600
Jiniu	Pelton	2	123	2890	506.5	300
Varahi II	Pelton	2	126.5	2910	460	300
Vishnupraguay	Pelton	1	120.4	2880	953.4	428.6
Jinwo	Pelton	2	143.6	2630	595	375
Rezonghai	Pelton	2	123	2550	560	375
Xi Luo Du	Francis	3	784	7655	197	125
GongGuoQiao	Francis	4	225	6760	66	93.75
JiangBian	Francis	3	110	2100	306.2	333.3
JiangPingHe	Francis	2	225	4030	178.89	187.5
XiGu	Francis	3	83	1560	431.4	500
Nam Ngum 2	Francis	3	209.2	4080	166.6	214.3
Kami-Shiiba	Francis	1	47.6	2630	144	300
Siguragura	Francis	2	73.2	2110	230.9	333
DaYiangJiang	Francis	4	175	2110	331	300
Li Yuan	Francis	4	612	8150	106	93.8
Da Gang Shian	Francis	4	663	7000	160	125
Ting Zi Kou	Francis	4	275	6640	73	100
Jing Ping II	Francis	8	610	6500	318.8	166.7
Nuo Zha Du	Francis	3	650	7250	215	125
An Khe	Francis	2	81.6	2518	377.5	500
Ji Shi Xia	Francis	3	340	7650	66	85.7
Yewa	Francis	4	195.5	4850	91.7	12.8
Si Lin	Francis	4	267.85	6810	64	93.75
Xiao Wan	Francis	3	700	6600	216	150
Xe Kaman III	Francis	2	127.55	1600	515.38	500
Nathpa Jhakri	Francis	4	336	2519	487	300
Karebbe	Francis	2	66.4	3284	73.6	200
Cheongpeyong	Kaplan	1	60	6400	22.3	102.9
Cao Jie	Kaplan	4	128.2	9500	20	68.18
Karnafuli	Kaplan	1	67.7	5607	32	115.38
<b>Australasia</b>						
Benmore	Francis	6	93.2	4085	93	166.7
Bogong	Francis	2	74.6	2050	419.3	600
Dartmouth	Francis	1	180		410	
Devils Gate	Francis	1	60			
Gordon River	Francis	3	144			
Murray-1	Francis	10	95			
Tumut - 3	Francis	6	250			
Clyde	Francis	4	108			
Agus II	Francis	3	60			
Pulangui	Francis	3	85			
<b>North - America</b>						
Noxon Rapids	Francis	3	115.8	5500	48.158	100
Folsom	Francis	3	66.2	3510	60	163.6
Gordon M Shrum	Francis	1	310	4870	152.4	150
Eastmain 1 A	Francis	3	260	6600	63	100

Picote II	Francis	1	248	6150	66.6	115.4
Abitibi	Francis	1	66.41	3520	72.5	150
Revelstoke	Francis	1	512	7100	127.1	112.5
Sir Adam Beck	Francis	8	55	3030	89	225
Des Joachimes	Francis	8	57.5	4470	40	105.9
Jocasse	Pump	2	208	7500	92	120
Rocky Mountain	Pump	3	370	4200	210	225
Holtwood	Kaplan	2	59.2	7150	15.5	85.7
Rainbow	Kaplan	1	62	5400	35.8	144
<b>South America</b>						
Parigo De Souza	Pelton	1	65	2700	754	514
El Platanal	Pelton	2	110	2190	608.7	450
Hornitos	Pelton	1	55.02	1910	561.56	500
Guri II	Francis	5	770	8000	136	112.5
Confluencia	Francis	2	81.6	1650	334.51	500
Serra Do Facao	Francis	2	108.2	3920	78.3	171.4
Mazar	Francis	2	80	3000	131.44	257.14
Salto Pilao	Francis	2	93	2650	194.9	360
Antuco	Francis	2	165	3150	196	250
Rapel	Francis	2	77	3500	75.5	187.5
Infiernillo	Francis	4	205	4735	114.5	163.64
La Villita	Francis	2	81.65	5000	46.41	120
Simplicio	Francis	3	104	3250	105.3	225
Macagua I	Francis	6	83	4900	46	120
Itaipu	Francis	20	715	8100	118.4	90.9
El Cajon	Francis	4	75	2475	156	300
Jirau	Kaplan	10	76.55	7500	15.2	94.7
Santo Antonio	Kaplan	13	71.05	7500	13.9	100
Estreito	Kaplan	8	138.65	9500	18.94	62.98
<b>Europe</b>						
Sedrun	Pelton	3	52	2150	588	428.6
Fionnay	Pelton	6	70	2650	872	428.6
Kaprun	Pelton	1	63	2255	868	500
Kjosnesfjorden	Pelton	1	84.1	1905	785	600
Uvdal	Pelton	2	53.72	1935	571.17	500
Florli	Pelton	1	88.3	1874	773.99	600
Zaramagaskaya	Pelton	2	171	3350	610	300
Akkoey II	Pelton	2	116.78	1940	1220	750
Naturno	Pelton	1	61.7	2700	1129	500
Lotru Ciunget	Pelton	3	170	3810	788	375
Grosio	Pelton	1	107	2970	600	333
Aguayo	Pump	1	85	3000	307	500
La Muela II	Pump	4	210	3180	494	600
Limberg II	Pump	2	240	3910	420	428.57
Obrovac	Pump	1	151.8	1137	541	600
Dez Dam	Francis	8	91.5	2490	164	250
Zakucac	Francis	4	150	2500	265	333.33
Uluabat	Francis	2	50	1850	292	600
Driva	Francis	1	81	2390	540	600
Mequinenza	Francis	4	83.5	5000	50	136.5
Orichella	Francis	1	75	2200	474	600
Akkoeproe	Francis	2	59.3	3150	86.8	214.3
Waldeck II	Francis	1	240	3350	325	375
Belesar	Francis	3	78	3110	120	214
Bemposta	Francis	1	193.5	5900	67.5	115.4
Hacininoglu	Francis	2	60.13	2382	140.24	300
Harspranget	Francis	1	122.6	3725	110	166.8
Kilforsen	Francis	1	105.74	3725	100	166.7
Feldsee	Francis	1	70.4	1912	524	1000

Songa	Francis	1	127	2304	264	300
Hintermuhr	Francis	1	74.85	1870	517.02	1000
Picote II	Francis	1	248	6150	66.6	115.4
Castrelo	Kaplan	2	56	6800	20	93.75
Ligga	Kaplan	3	185	7500	39	107.14
Cachoeira Dourada	Kaplan	1	55.45	5540	34.5	128.6
Akkats	Kaplan	2	75	5200	42.6	166.7
Uglich	Kaplan	1	70	9000	14.5	600
Vardinili I	Kaplan	1	73.3	4000	59	187.5
<b>Africa</b>						
Gilgel Gibe II	Pelton	4	105	2580	485	333
Ingula	Pump	4	342	4260	441	428.6
Drakensberg	Pump	4	250			
Afourer	Pump	2	176		594	
Kiambere	Francis	2	84	2700	153.7	300
Beles	Francis	4	119.4	1900	320	375
Shiroro	Francis	4	155	4460	97	150
Aswan High Dam	Francis	2	175		74	100
Merowe	Francis	10	125		43	
Cahora Bassa	Francis	5	415			
Turkwell	Francis	2	57.5		364	





# Appendix D.3: Dia00

Assumed      Given      Rules      Calculated

### Known data:

Nominal output	$P_n$	MW	82
Rotation speed	$n$	rpm	230.8
Nominal volume flow	$Q_n$	$m^3/s$	68
Gravity constant	$g$	$m^2/s$	9.78
Density	$\rho$	$kg/m^3$	997
Pådragskoeff	$\kappa$		1.15
Inlet diameter	$D_1$	m	3.312
Outlet diameter	$D_2$	m	2.94
	$B_0$	m	0.65
	$B_1$	m	0.649
Angular velocity	$\omega$	rad/s	24.17

<b>Increase D2</b>	<b>By</b>	<b>m</b>	<b>0</b>
	<b>New</b>	<b>m</b>	<b>2.94</b>
Area outlet	$A_2$	$m^2$	6.79
Safety factor			0.15
	$NPSH_A$	m	16.9

Subtract from NPSH		0	0.1	0.2	1	0.4	0.5
$NPSH_T$	m	14.3	14.2	14.1	13.3	13.9	13.8
a		1.12					
b		0.060	0.060	0.059	0.058	0.059	0.059
$u_2$	m/s	35.5					
$\underline{u}_2$		0.72					
$\beta_2$	rad	0.29	0.29	0.29	0.28	0.29	0.28
	deg	16.71	16.63	16.55	15.90	16.39	16.31
* $\Omega$		0.60	0.60	0.59	0.58	0.59	0.59
* $c_{m2}$	m/s	10.66	10.61	10.56	10.12	10.45	10.40
* $c_{u2}$		0	0	0	0	0	0
		OK	OK	OK	OK	OK	OK
* $Q$		72.39	72.03	71.67	68.71		
$Q_n$	$m^3/s$	83.25	82.83	82.42	79.02		
		OK	OK	OK	OK		
Increase	%	22	22	21	16		
$c_{m2}$	m/s	12.26	12.20	12.14	11.64		
$NPSH_{T_{new}}$	m	12.47	12.37	12.28	11.51		
		OK	OK	OK	OK		

Nominal Head (Retrieved from Matlab)	$H_n$	m	123.3	123.6	123.9	126
---	-------	---	-------	-------	-------	-----

<b>Assumed Efficiency</b>	$\eta_H$		<b>0.93</b>				
	$P_{new}$	MW	93.08	92.84	92.60	90.29	
	$P_{new} - P_{old}$	MW	11	11	11	8	
	Increase	%	13.51	13	13	10	

<b>Assumed Efficiency</b>	$\eta_H$	<b>0.94</b>				
	$P_{new}$	MW	94.08	93.84	93.59	91.26
	$P_{new} - P_{old}$	MW	12	12	12	9
	Increase	%	14.73	14	14	11

<b>Assumed Efficiency</b>	$\eta_H$	<b>0.95</b>				
	$P_{new}$	MW	95.08	94.84	94.59	92.23
	$P_{new} - P_{old}$	MW	13	13	13	10
	Increase	%	15.95	16	15	12

## Appendix D.6: Dia06

Assumed	Given	Rules	Calculated						
<b>Known data:</b>									
Nominal output	$P_n$	MW	82						
Rotation speed	$n$	rpm	230.8						
Nominal volume flow	$Q_n$	$m^3/s$	68						
Gravity constant	$g$	$m^2/s$	9.78						
Density	$\rho$	$kg/m^3$	997						
Pådragskoeff	$\kappa$		1.15						
Inlet diameter	$D_1$	m	3.312						
Outlet diameter	$D_2$	m	2.94						
	$B_0$	m	0.65						
	$B_1$	m	0.649						
Angular velocity	$\omega$	rad/s	24.17						
<b>Increase D2</b>	<b>By</b>	<b>m</b>	<b>0.06</b>						
	<b>New</b>	<b>m</b>	<b>3</b>						
Area outlet	$A_2$	$m^2$	7.07						
Safety factor			0.15						
	$NPSH_A$	m	16.9						
	Subtract from NPSH		0	0.1	0.2	0.3	0.4	0.5	
	$NPSH_T$	m	14.3	14.2	14.1	14.0	13.9	13.8	
	a		1.12						
	b		0.061	0.061	0.061	0.060	0.060	0.060	
	$u_2$	m/s	36.3						
	$\underline{u}_2$		0.74						
	$\beta_2$	rad	0.28	0.28	0.28	0.28	0.28	0.27	
		deg	16	16	16	16	16	16	
	* $\Omega$		0.61	0.61	0.61	0.60	0.60	0.60	
	* $c_{m2}$	m/s	10.45	10.40	10.34	10.29	10.23	10.18	
	* $c_{u2}$		0	0	0	0	0	0	
			OK	OK	OK	OK	OK	OK	
	* $Q$		73.86	73.48	73.10	72.72			
	$Q_n$	$m^3/s$	84.94	84.50	84.06	83.63			
			OK	OK	OK	OK			
	Increase	%	25	24	24	23			
	$c_{m2}$	m/s	12.02	11.95	11.89	11.83			
	$NPSH_{T_{new}}$	m	12.36	12.26	12.17	12.07			
			OK	OK	OK	OK			
Nominal Head (Retrieved from Matlab)	$H_n$	m	122.0	122.4	127.7	123.0			
<b>Assumed Efficiency</b>	$\eta_H$		<b>0.93</b>						
	$P_{new}$	MW	93.97	93.79	97.35	93.27			
	$P_{new} - P_{old}$	MW	12	12	15	11			
	Increase	%	15	14	19	14			

<b>Assumed Efficiency</b>	$\eta_H$	<b>0.94</b>				
	$P_{new}$	MW	94.98	94.80	98.39	94.28
	$P_{new} - P_{old}$	MW	13	13	16	12
	Increase	%	15.82	16	20	15

<b>Assumed Efficiency</b>	$\eta_H$	<b>0.95</b>				
	$P_{new}$	MW	95.99	95.81	99.44	95.28
	$P_{new} - P_{old}$	MW	14	14	17	13
	Increase	%	17	17	21	16

## Appendix D.7: Calculation of potential increase in power output (Sintef)

Assumed	Given	Rules	Calculated	
Nominal volume flow	$Q_n$	$m^3/s$	68	
Nominal output	$P_n$	MW	82	
Nominal Head	$H_n$	m	121.9	
Rotation speed	$n$	rpm	230.8	
Gravitation	$g$	$m^2/s$	9.78	
Outlet diameter	$D_2$	m	2.94	3.00
Density	$\rho$	$kg/m^3$	997	
Hydraulic efficiency	$\eta_H$		0.95	

		Sintef00	Sintef06
<b>Assume increase in output</b>	%	<b>17.00</b>	<b>17.00</b>
	$P_{increase}$ MW	95.94	95.94
	$Q_{increase}$ $m^3/s$	84.96	84.96
		25	25

### Calculations:

Pådragskoeff	$\kappa$	1.15	1.15
Best volume flow	$*Q$ $m^3/s$	73.9	73.9
Increase		9	9
Angular velocity	$\omega$ rad/s	24.2	24.2
Speed number	$\Omega$	0.609	0.609
Specific speed	$n_s$	1.0	1.0
Outlet area	$A_2$ $m^2$	6.8	7.1

### Best operating point

Meridian velocity BEP	$*c_{m2}$ m/s	10.9	10.5
Periferal velocity	$u_2$ m/s	35.5	36.3
Outlet angle	$\beta_2$ rad	0.3	0.3
	deg	17.0	16.1

### Nominal load

$w_2$  and  $c_{m2}$  increases while  $\beta_2$  remains the same

Meridian velocity	$c_{m2}$ m/s	12.5	12.0
Tangential velocity	$c_{u2}$ m/s	5.3	5.4

### Net Positive Suction Head

	a	1.12	1.12
	b	0.061	0.061
	$NPSH_T$ m	12.9	12.4
	$NPSH_A$ m	14.4	14.4
Is the cavitation criteria fulfilled?:		YES	YES

### Calculation of increased output

The geometry must be changed in order to allow more water

$NPSH_T$  Constant

#### Case 1:

Draft tube	$D_{22}$ m	2.94	3
New possible diameter	$D'_2$ m	2.94	3

#### Case 2:

New possible diameter	$D''_2$	m	3.328	3.396
-----------------------	---------	---	-------	-------

The smallest diameter will be chosen

$D_{2new}$	m	2.94	3
------------	---	------	---

**Which case scenario?**

<b>Case 1</b>	<b>Case 1</b>
---------------	---------------

Checking cavitation	$C_{m2new}$	m/s	12.5	12.0
	$u_{2new}$	m/s	35.5	36.3
	$NPSH_{Tnew}$	m	12.9	12.4

<b>Is the cavitation criteria fulfilled?:</b>	<b>YES</b>	<b>YES</b>
---	------------	------------

**New values**

Volume flow	$Q_{new}$	$m^3/s$	85.0	87.6
-------------	-----------	---------	------	------

Output	$P_{new}$	MW	95.9	98.9
--------	-----------	----	------	------

reduced head factor	$\epsilon_h$	1		
---------------------	--------------	---	--	--

<b>Output</b>	$P_{new,f}$	<b>MW</b>	<b>95.9</b>	<b>98.9</b>
---------------	-------------	-----------	-------------	-------------

$P_{new}-P_n$		<b>MW</b>	<b>13.9</b>	<b>16.9</b>
		<b>%</b>	<b>15</b>	<b>18</b>